Optical and Radio Frequency Observations of Twenty Long Period Variable (LPV) Astrophysical Masers

Abstract Astrophysical masers are naturally occurring sources of stimulated spectral line emission, typically in the microwave frequency range of the electromagnetic spectrum. The emission from a maser is stimulated, having the frequency corresponding to the energy difference between two quantum-mechanical energy levels of the molecular species in the gain medium which have been pumped into a non-thermal population distribution. Typical molecules that can produce astrophysical maser emissions include, OH (hydroxyl), water, ammonia, and SiO (silicon monoxide). In the case of SiO, the stimulated frequency is in the 43 GHz frequency band (42373.341-43423.853 GHz, depending on the specific isotope). Observations of SiO masers at 43 GHz will be discussed below. These radio frequency observations will be correlated with the phases of twenty Long Period Variable (LPV) stars that have extensive optical light curves utilizing Johnson-Cousins photometry.

1. Introduction and Background

The American Association of Variable Star Observers, (AAVSO) **(**Kloppenborg 2022, American Association of Variable Star Observers (https://aavso.org)) and the University of New Mexico (Stroh, M. "Circumstellar SiO Masers in the Bulge Asymmetries and Dynamical Evolution Survey" 2019, https://digitalrepository.unm.edu/phyc_etds/216) participated in a cooperative effort to study SiO maser emissions in Long Period Variable (LPV) stars. The maser emissions were observed with the Jansky Very Large Array (JVLA) by the University of New Mexico and the corresponding optical light curves were taken from the AAVSO International Variable Star Index (VSX) (Kloppenborg 2022, American Association of Variable Star Observers International Variable Star Index (https://www.aavso.org/vsx/)). In total, twenty Mira LPV stars were studied with the combination of the light curves and the 43 GHz radio frequency observations. The particular stars selected were based on previous SiO observations as well as a good history of AAVSO coverage. These objects are outlined in Figure 1.

BAaDE Name	Associated Name	R.A. (J2000)	Declination (J2000)	Period (days)	Variable Classification	Previous SiO v=3 Detection?
ad3a-18267	TY Cas	00:36:59.42	+63:08:01.7	645	Mira	No
ad3a-17750	FI Per	03:54:56.75	+48:36:01.9	427	Mira	Yes
ad3a-13536	SY Mon	06:37:31.34	-01:23:43.0	423	Mira[a]	No
ad3a-15213	FX Mon	06:45:05.60	+09:02:18.5	428	Mira	No
ad3a-13321	NSVS 12572573	06:45:14.95	-02:26:35.1	375	Mira	Yes
ad3a-16553	V0349 Vul	19:31:10.47	+23:30:33.5	363	Mira	Yes
ad3a-15617	RT Aql	19:38:01.61	+11:43:18.3	327	Mira	No
ad3a-16500	V0353 Vul	19:49:22.06	+22:37:39.8	470	Mira	Yes
ad3a-16952	SX Cyg	20:15:33.53	+31:04:20.1	411	Mira	No
ad3a-17123	AU Cyg	20:18:32.77	+34:23:20.5	435	Mira	Yes
ad3a-17332	V1655 Cyg	20:25:24.02	+38:42:35.6	462	Mira	Yes
ad3a-17830	NSVS J2041274+511326	20:41:27.45	+51:13:29.8	350	Mira	Yes
ad3a-17304	DR Cyg	20:43:41.01	+38:09:56.1	314	Mira	No
ad3a-17802	V0750 Cyg	20:49:21.17	+50:31:51.3	433	Mira	No
ad3a-18063	W Cep	22:36:27.57	+58:25:34.0	350	SRc	Yes
ad3a-18292	VX Cep	22:50:49.45	+64:15:04.7	532	Mira	Yes
ad3a-18081	V0850 Cas	23:37:39.74	+58:50:45.9	365	SR	No
ad3a-18070	AL Cep	22:49:16.89	+58:35:07.1	277	Mira	No
ad3a-18128	V Cas	23:11:40.71	+59:41:58.7	229	Mira	No
ce3a-00250	V0657 Cas	23:52:04.92	+61:48:12.4	607	Mira	Yes

Positions are from the 2MASS associated position. Associated name, period, and variable classification are taken from the VSX catalog (Watson et al., 2006). The last column lists whether SiO v=3 emission was found in the original VLA BAaDE observations. [a]This object is also classified as an OH/IR star (Sivagnanam et al., 1988; Szymczak & Le Squeren, 1999).

Figure 1: Twenty SiO Masers Selected (Courtesy M. Stroh)

1.1 Maser Physics and SiO Spectra

The physics of masers, including astrophysical masers is illustrated in Figure 2. The stimulated emission of radiation begins with a molecule in a non-excited state (A). The molecule is excited due to a pumping mechanism that may be due to collisions and/or radiation (B). The molecule is then de-excited to a meta-stable state (C) and an incident photon with the energy equal to the energy of the transition stimulates the molecule causing de-excitation (D). Due to the de-excitation, an additional photon is emitted with the same energy as the incident photon (E).

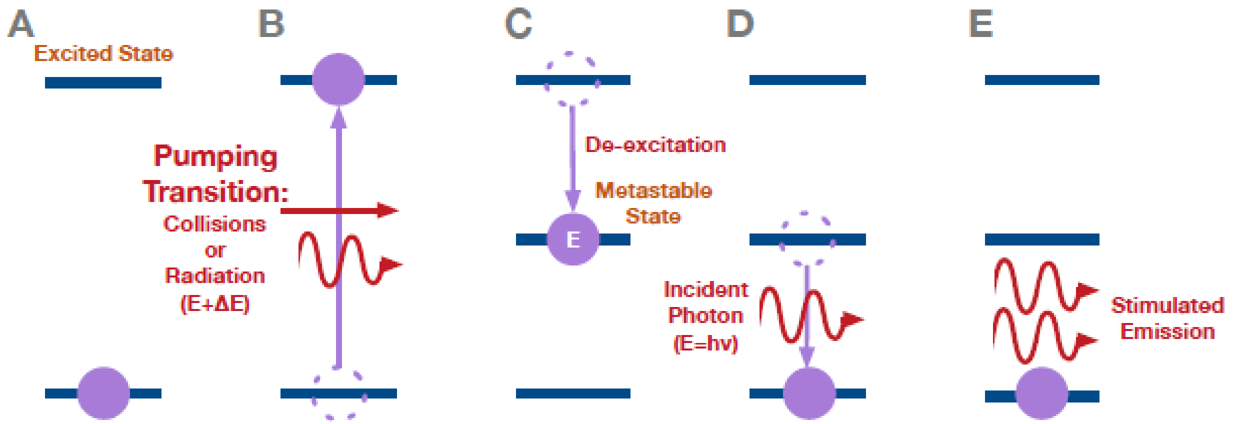

Figure 2: Stimulated Emission of Radiation (Courtesy M. Stroh)

Figure 3 shows the SiO energy levels for the 43 GHz radio frequency signal. SiO maser emission is associated with rotational de-excitation within vibrational states, with the 43 GHz SiO maser lines for the J = 1-0 transitions (42373.341-43423.853 GHz, depending on the specific isotope). Figure 4 shows an example of a JVLA observation around 43 GHz.

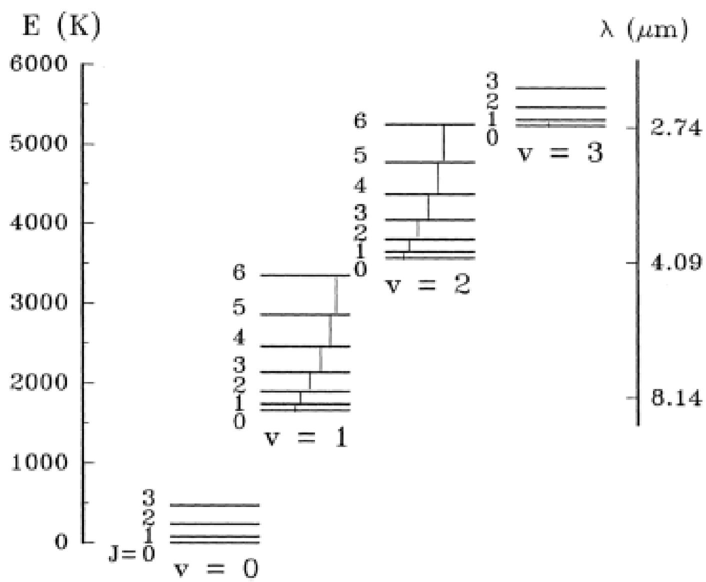

Figure 3: SiO Energy Level Diagram (Elitzur 1992)

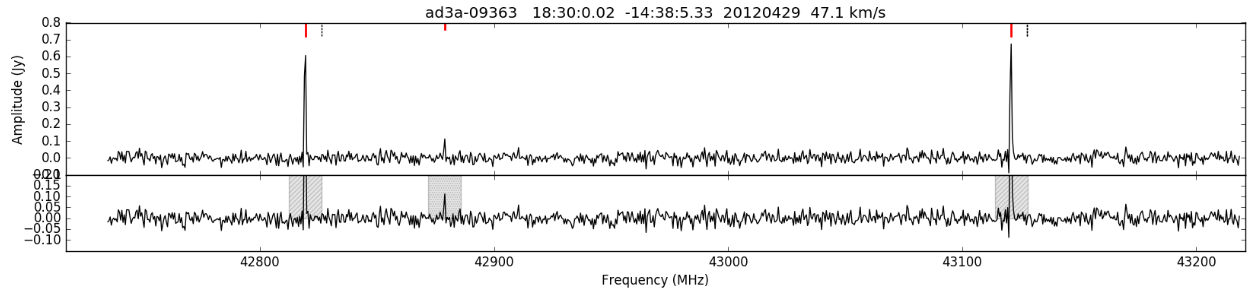

Figure 4: A Sample SiO Maser Spectra with Detection of the 28SiO(1-0) v=1 and v=2 Transitions, and a Weaker Detection of the 29SiO(1-0) v=0 Line. (Courtesy M. Stroh)

1.2 Mira Variable Stars and Optical Photometry

Mira or M stars are Ceti-type variables. These are long-period variable giants with a characteristic late-type emission spectra and light amplitudes from 2.5 to 11 magnitude in the optical V-band (500-700 nanometer wavelength). Their periodicity is well pronounced and the periods lie in the range between 80 and 1000 days. The periods of the twenty Mira SiO masers discussed herein lie between 229 and 645 days. The photometric system employed by the AAVSO for observations in the International Variable Star Index (VSX) is the Johnson-Cousins BVRI system. Johnson B (blue) is in the 400-500 nanometer wavelength range, Johnson V (visual) is in the 500-700 nanometer range, Cousins R (red) is in the 550-800 nanometer range, and Cousins I (infrared) is in the 700-900 nanometer range. The Johnson V or visual is in the optical spectrum to which the human eye is most sensitive.

2. Methods and Results

The data presented below include the latest complete optical light curve of each LPV maser object in Table 1 from the AAVSO Variable Star Index. Additionally, each object has a clickable direct link to VSX with all of the information in the AAVSO database about that star. Also shown is the portion of the optical light curve that is correlated with the time period of 43 GHz VLA observations (JD 2458249-JD 2458750 or May 10, 2018-September 23, 2019). Finally, the 43 GHz VLA data is shown which includes the AAVSO (and other) optical magnitude plots (a), the integrated flux density of the emission (b), the integrated flux density relative to the SiO v=1 emission (c), the velocity centroid of the emission (d), and the full linewidth at zero maximum, i.e., the width of all emissions (e).

The AAVSO light curves were generated and analyzed by the VStar software (Benn, D. 2012, “Algorithms + Observations = VStar”, JAAVSO, v40, n2, pp.852-866 (https://www.aavso.org/vstar)). VStar is a multi-platform variable star data visualization and analysis tool. Specifically, Fourier analysis of the photometric data was performed to yield a detailed periodogram for each of the twenty maser objects from which periodicities and other variations can potentially be identified. VStar utilizes the Date Compensated Discrete Fourier Transform (DCDFT) algorithm (Ferraz-Mello 1981) to produce a power spectrum, a period range, and a resolution. The Date Compensated DFT compensates for gaps in the data, which is common for variable star observations. The resulting analysis can include one or more periods and one or more harmonics. These can be selected to create a model that can also include a polynomial function that is used as a smoothing mechanism to capture key aspects of the data set without all the noise and fine fluctuations. When a model is created, it is subtracted from observations in the series to yield a second series called residuals. The residuals can also be analyzed to look for other signals (periods) in a process called pre-whitening. Periodicities and other potential variations were analyzed utilizing BVRI photometry, models were created from the photometry, mean series computed, and residuals analyzed to obtain all possible variations. In this particular case, the periodicities are not as important as they are normally for variable star research. Rather, the observation time overlap between the optical light curve data and the 43 GHz VLA data is the important feature. Optical and radio frequency data for all maser objects is presented below.

TY Cas

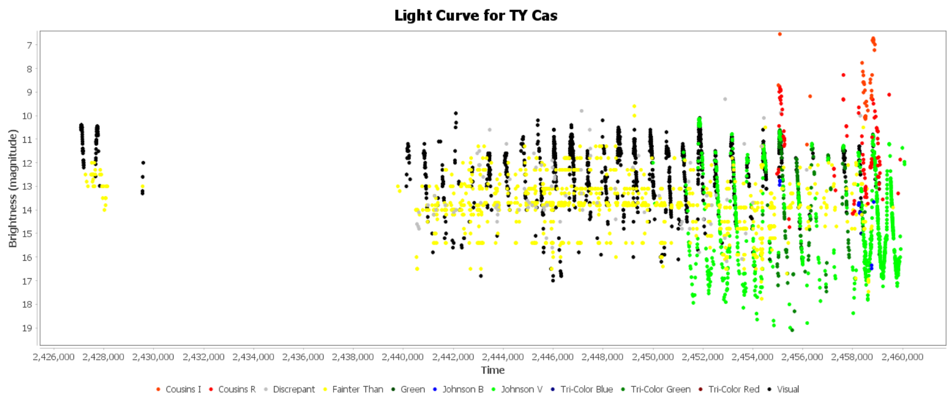

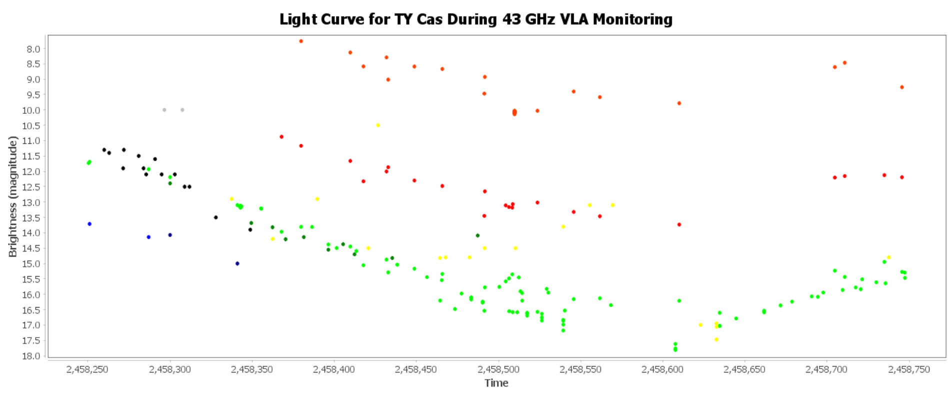

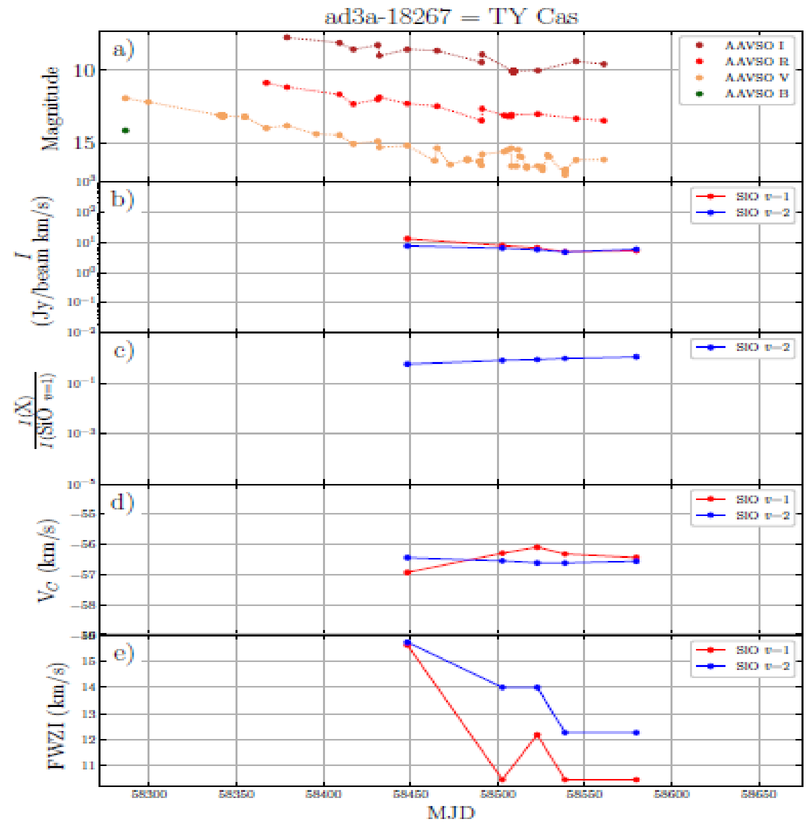

FI Per

Light Curve for FI Per

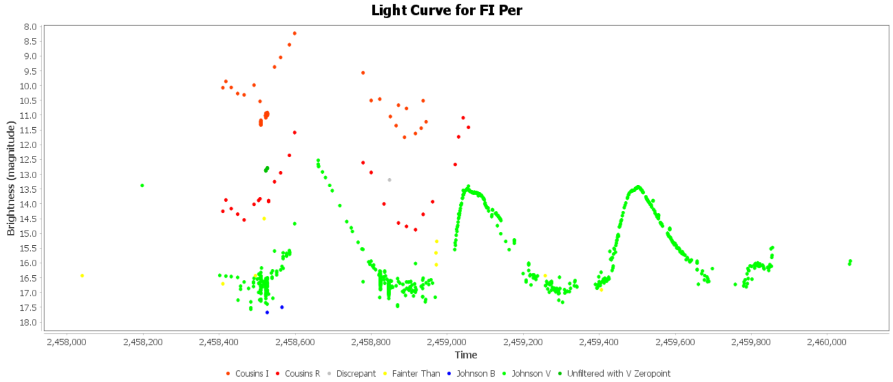

Light Curve for FI Per During 43 GHz VLA Monitoring

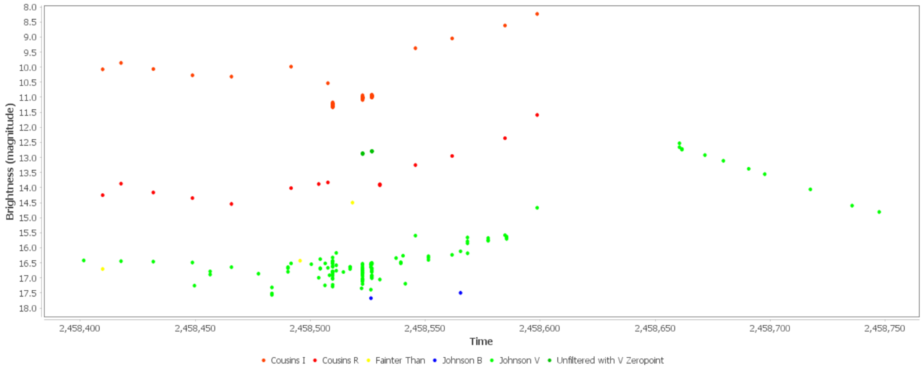

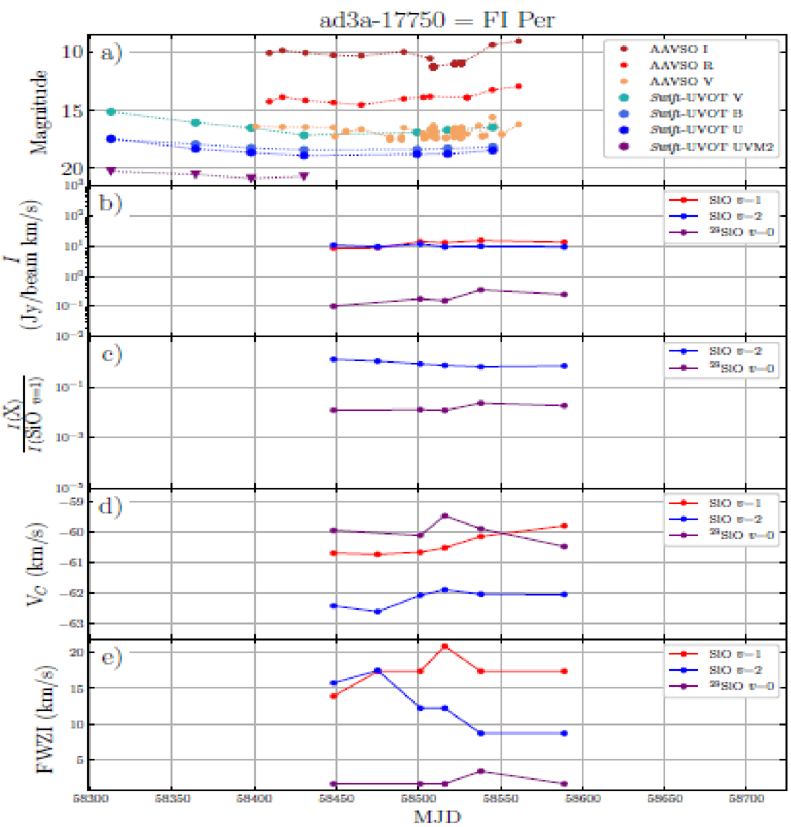

SY Mon

Light Curve for SY Mon

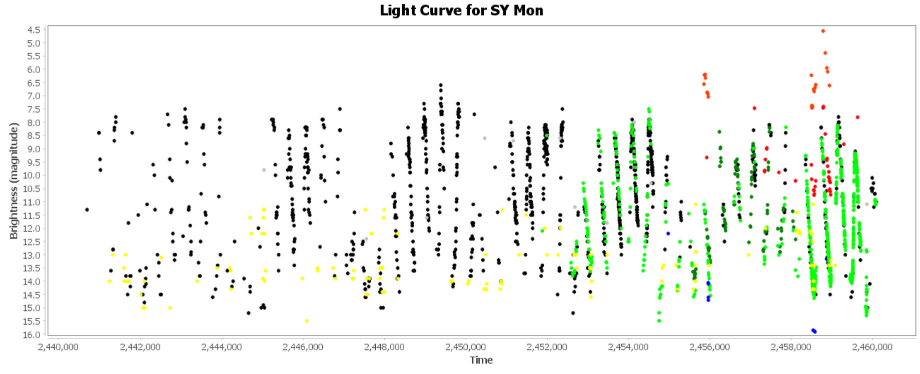

Light Curve for SY Mon During 43 GHz VLA Monitoring

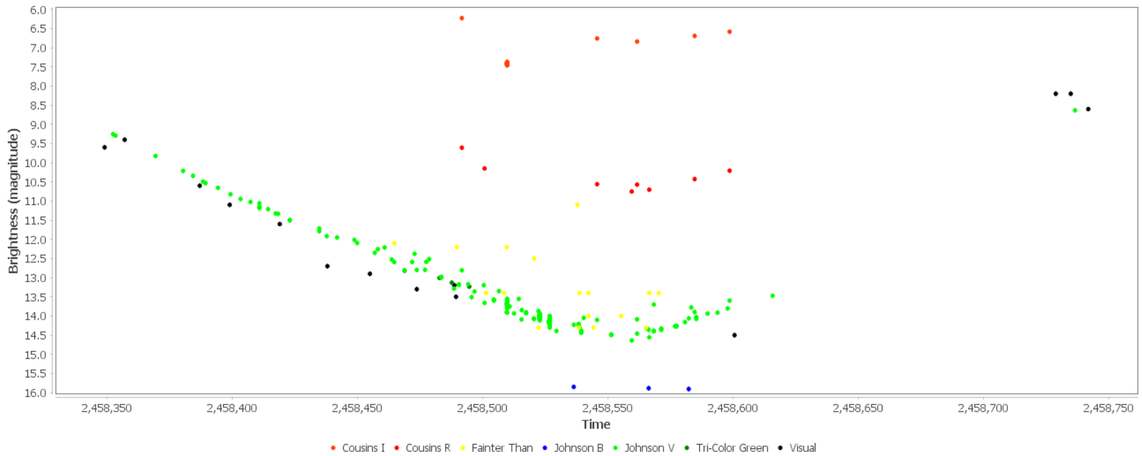

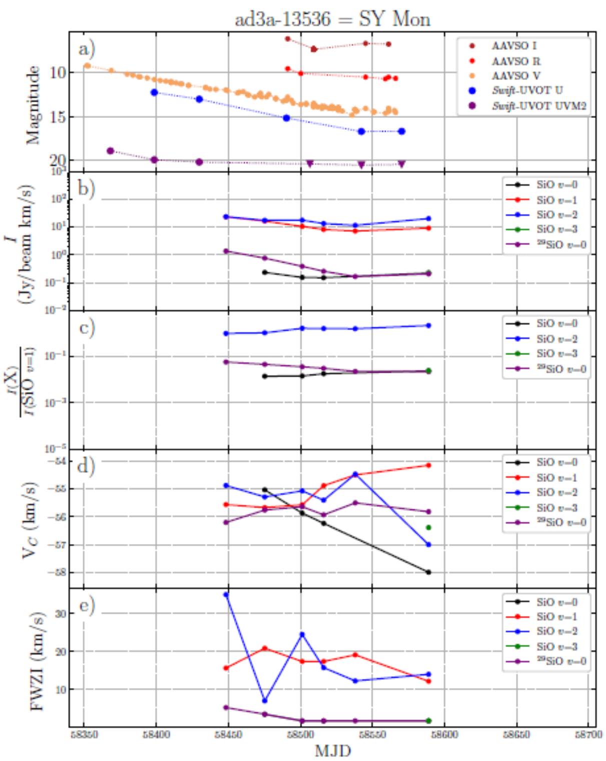

FX Mon

Light Curve for FX Mon

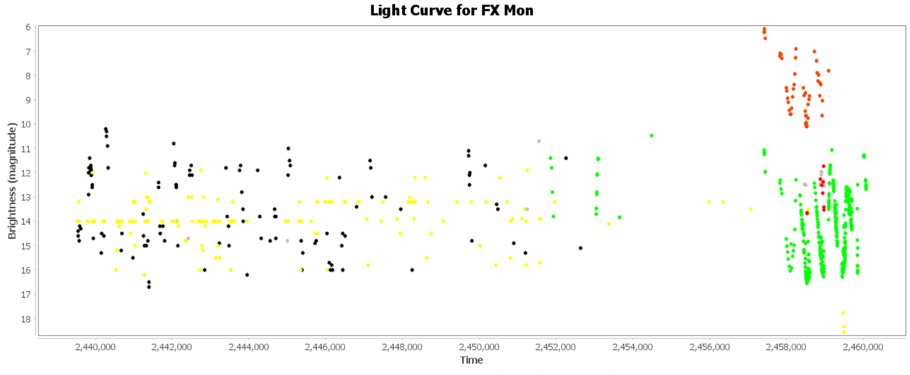

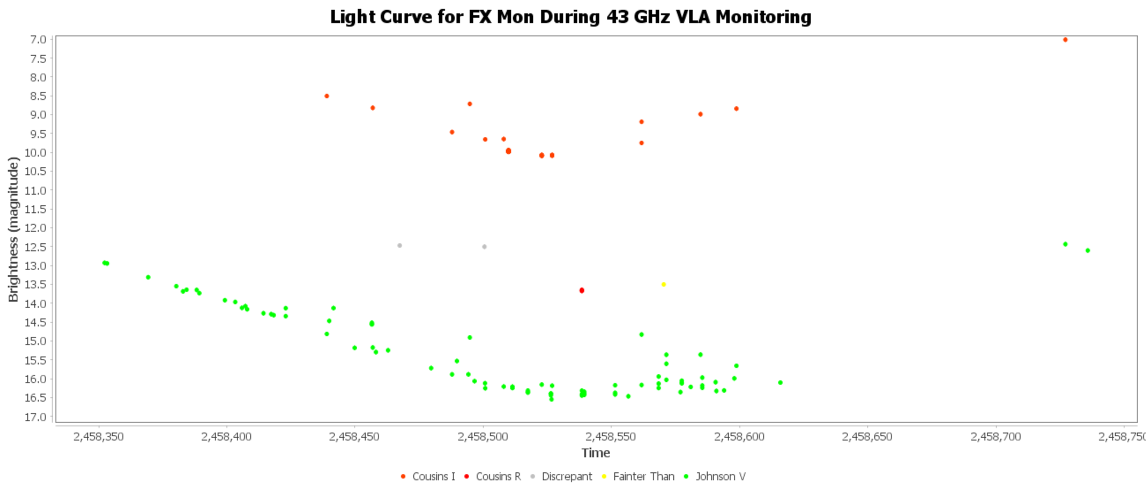
Light Curve for FX Mon During 43 GHz VLA Monitoring
Brightness (magnitude)
Time
Cousins I
Cousins R
Discrepant
Fainter Than
Johnson V

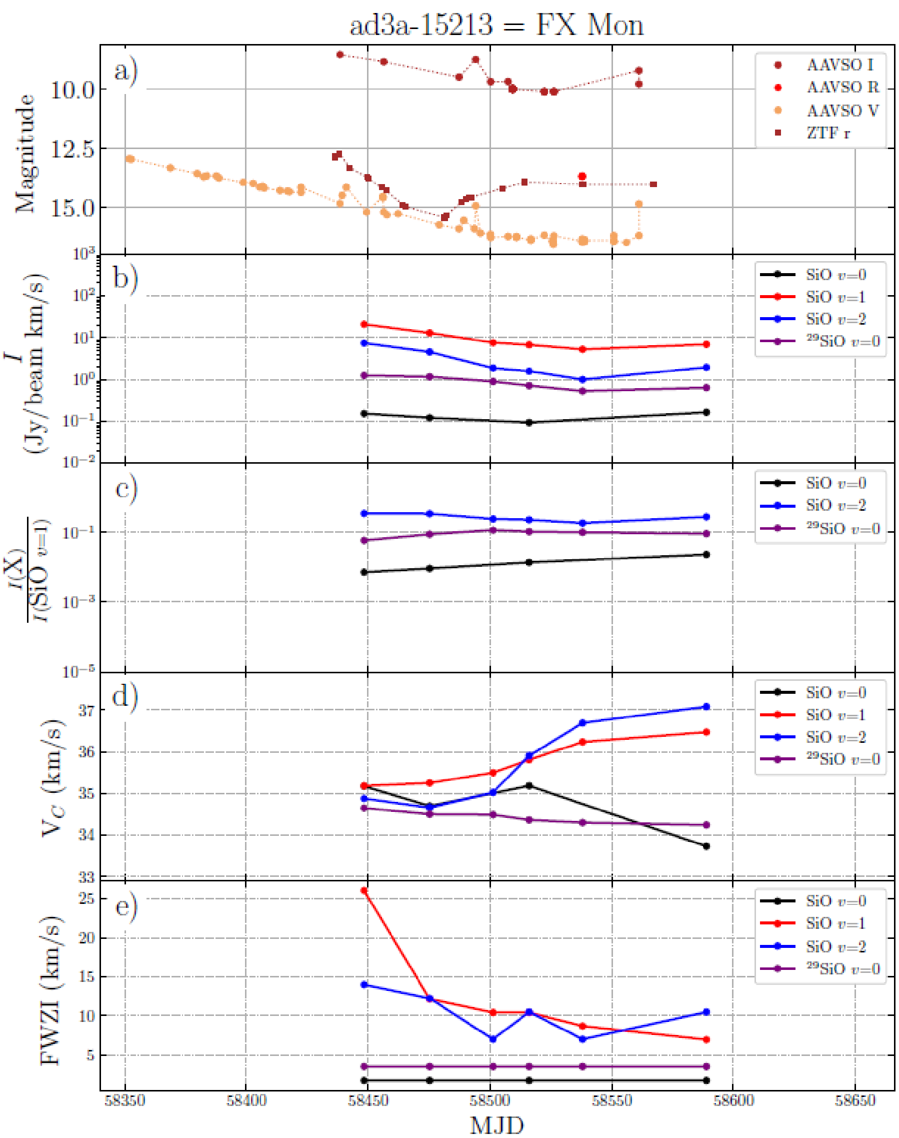
ad3a-15213 = FX Mon
a)
Magnitude
AAVSO I
AAVSO R
AAVSO V
ZTF r
b)
I (Jy/beam km/s)
SiO v=0
SiO v=1
SiO v=2
29SiO v=0
c)
I(X) / I(SiO v=1)
d)
V_C (km/s)
e)
FWZI (km/s)
MJD

NSVS 12572573

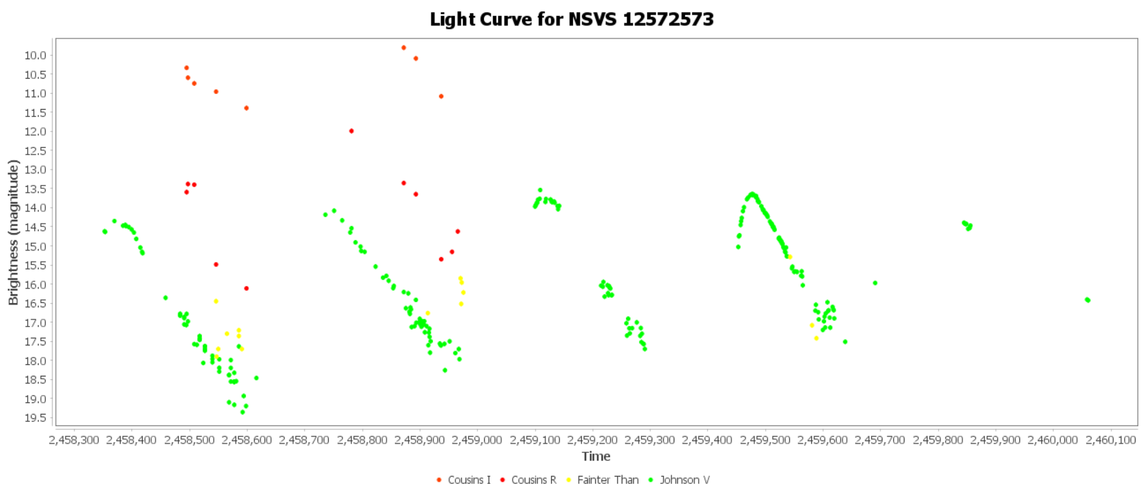

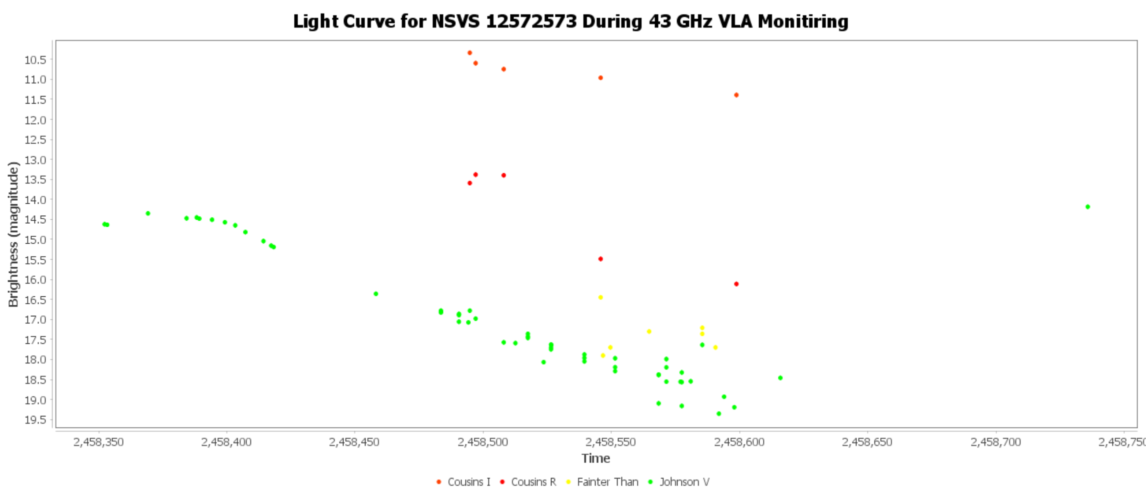

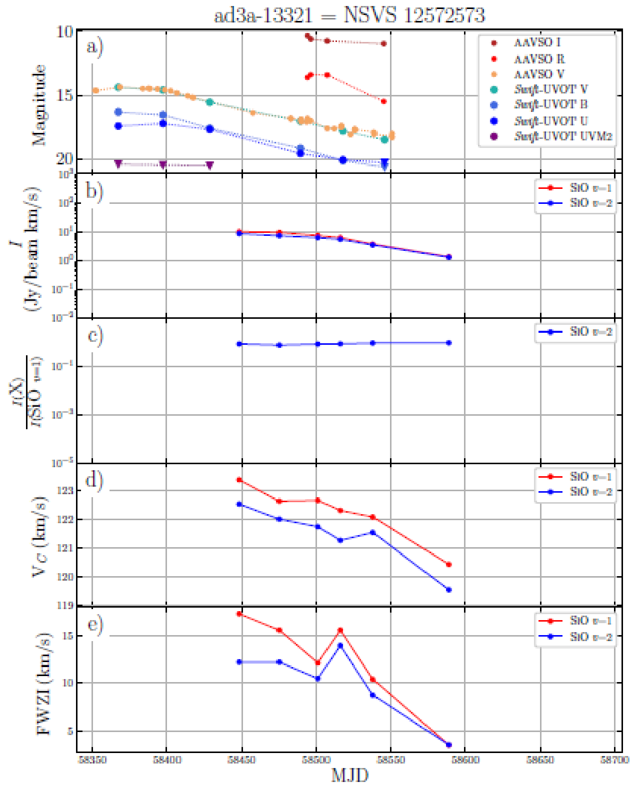
ad3a-13321 = NSVS 12572573
a)
Magnitude
AAVSO I
AAVSO R
AAVSO V
Swift-UVOT V
Swift-UVOT B
Swift-UVOT U
Swift-UVOT UVM2
b)
I (Jy/beam km/s)
SiO v=1
SiO v=2
c)
I(X) / I(SiO v=1)
SiO v=2
d)
V_C (km/s)
SiO v=1
SiO v=2
e)
FWZI (km/s)
SiO v=1
SiO v=2
MJD

V0349 Vul

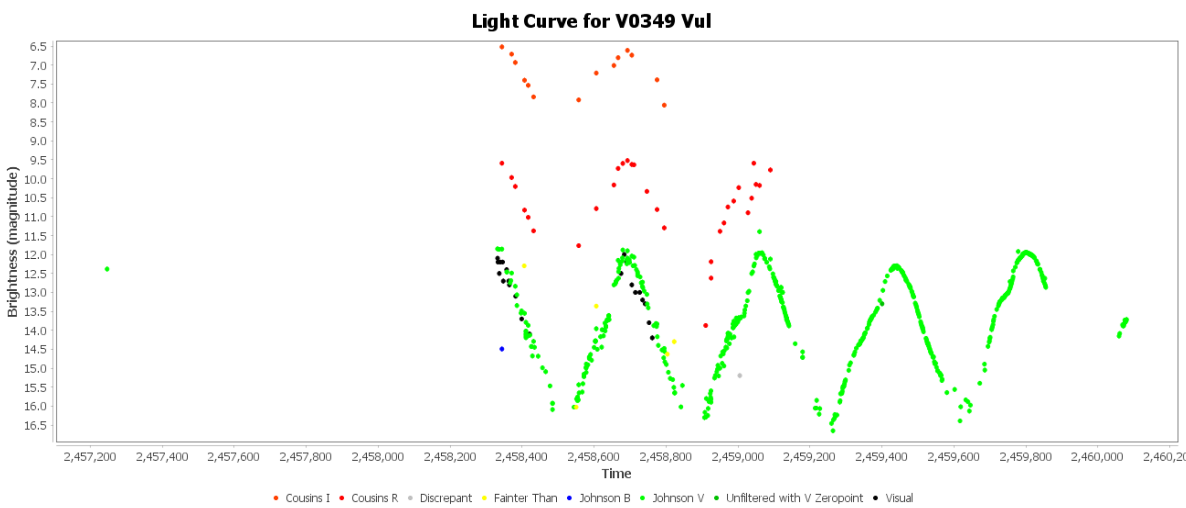
Light Curve for V0349 Vul
Brightness (magnitude)
Time
Cousins I
Cousins R
Discrepant
Fainter Than
Johnson B
Johnson V
Unfiltered with V Zeropoint
Visual

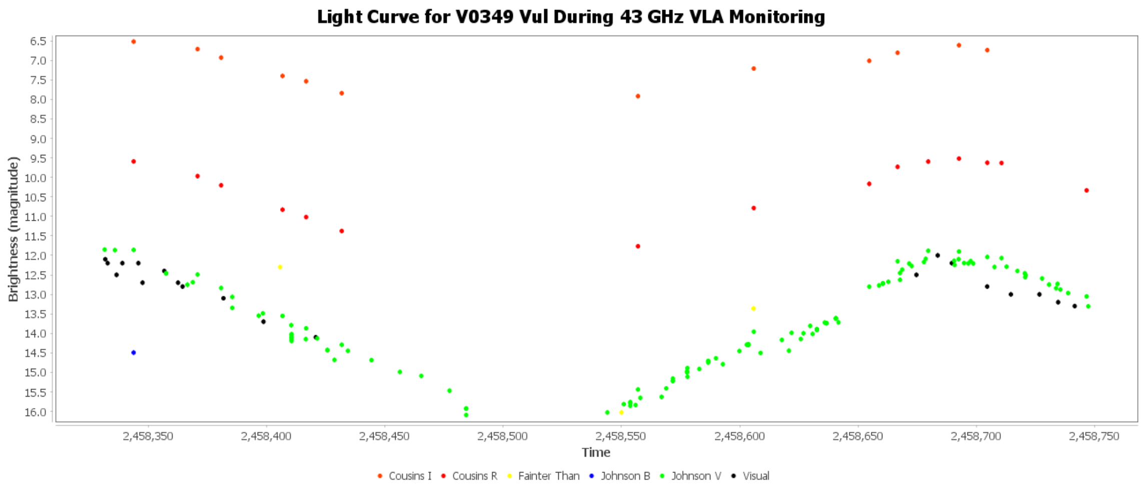
Light Curve for V0349 Vul During 43 GHz VLA Monitoring
Brightness (magnitude)
Time
Cousins I
Cousins R
Fainter Than
Johnson B
Johnson V
Visual

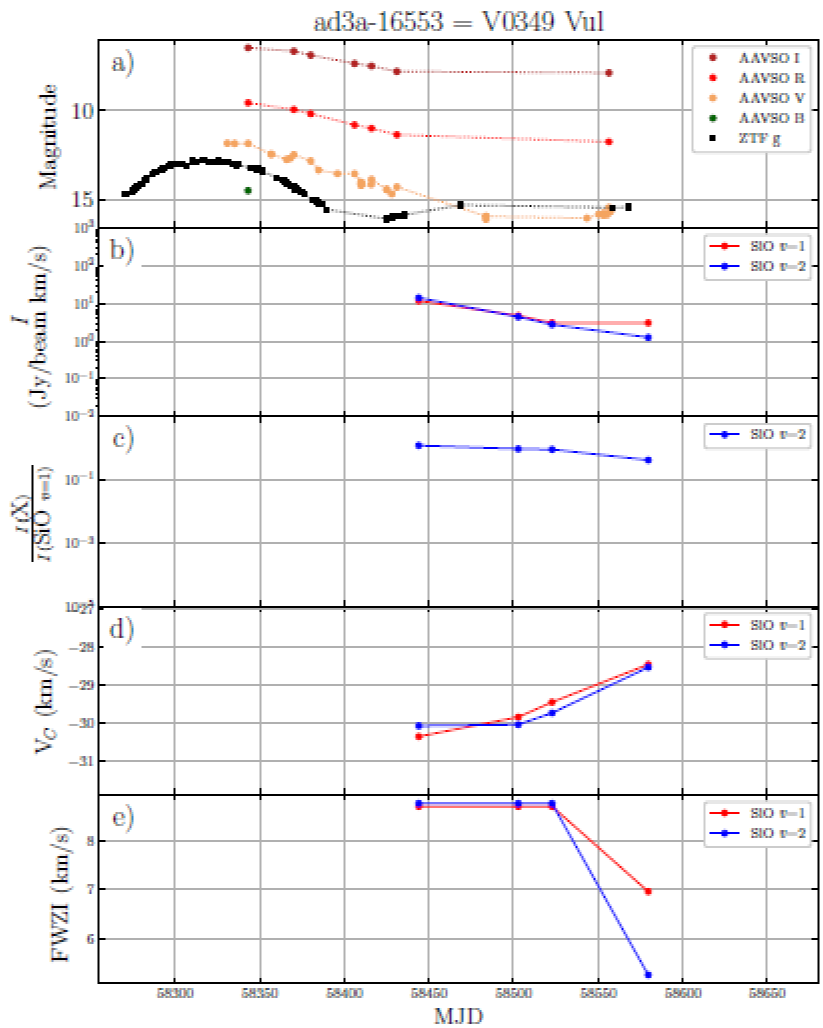
ad3a-16553 = V0349 Vul
a)
Magnitude
AAVSO I
AAVSO R
AAVSO V
AAVSO B
ZTF g
b)
I (Jy/beam km/s)
SiO v=1
SiO v=2
c)
I(X) / I(SiO v=1)
SiO v=2
d)
V_C (km/s)
SiO v=1
SiO v=2
e)
FWZI (km/s)
SiO v=1
SiO v=2
MJD

RT Aql

Light Curve for RT Aql

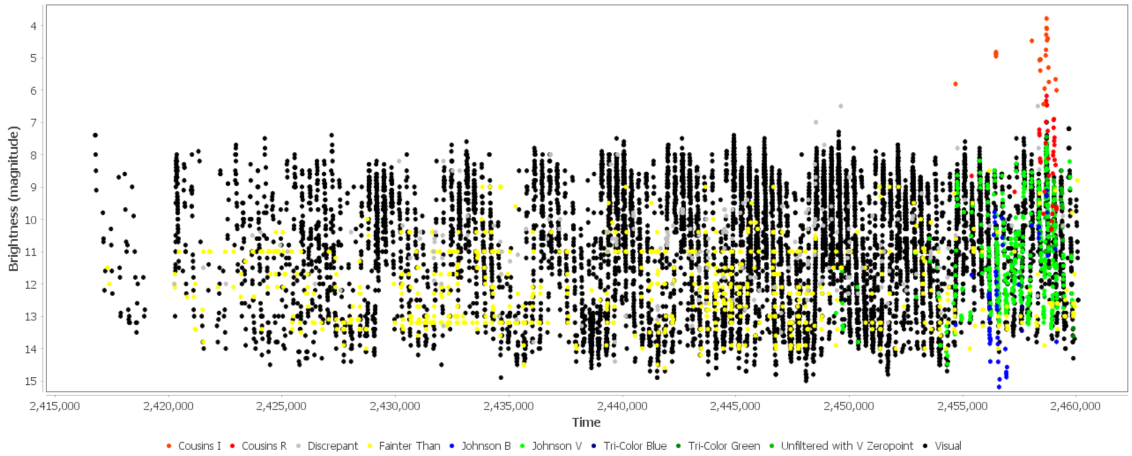

Light Curve for RT Aql During 43 GHz VLA Monitoring

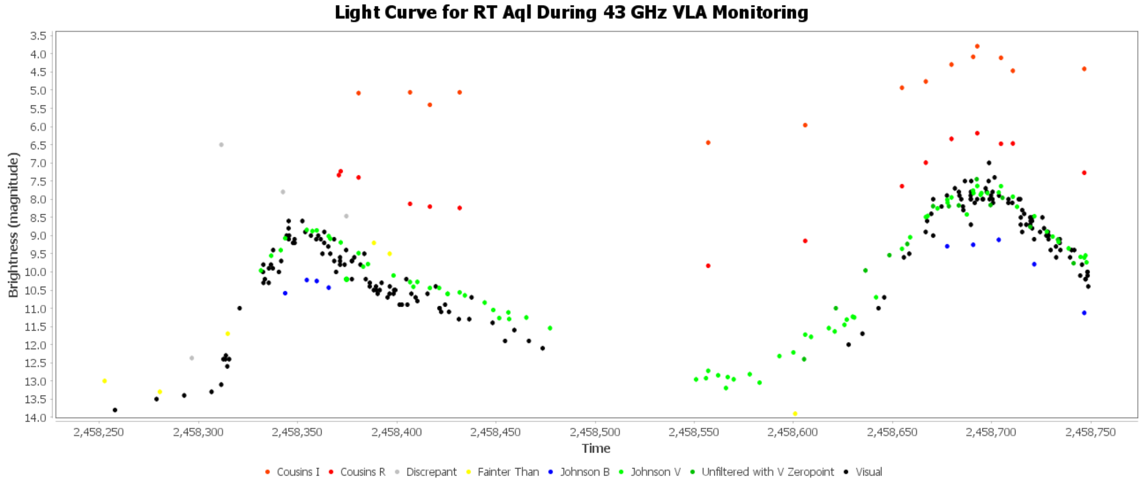

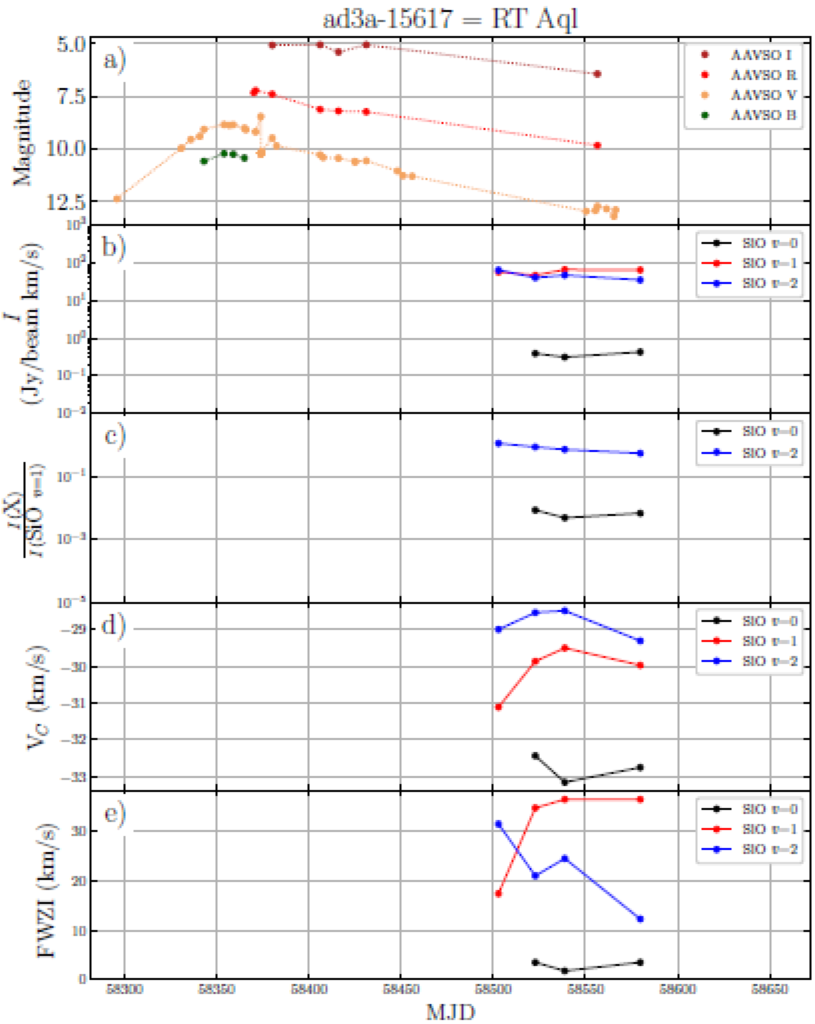
ad3a-15617 = RT Aql
Magnitude
AAVSO I
AAVSO R
AAVSO V
AAVSO B
I (Jy/beam km/s)
SiO v=0
SiO v=1
SiO v=2
I(X) / I(SiO v=1)
V_C (km/s)
FWZI (km/s)
MJD

V0353 Vul

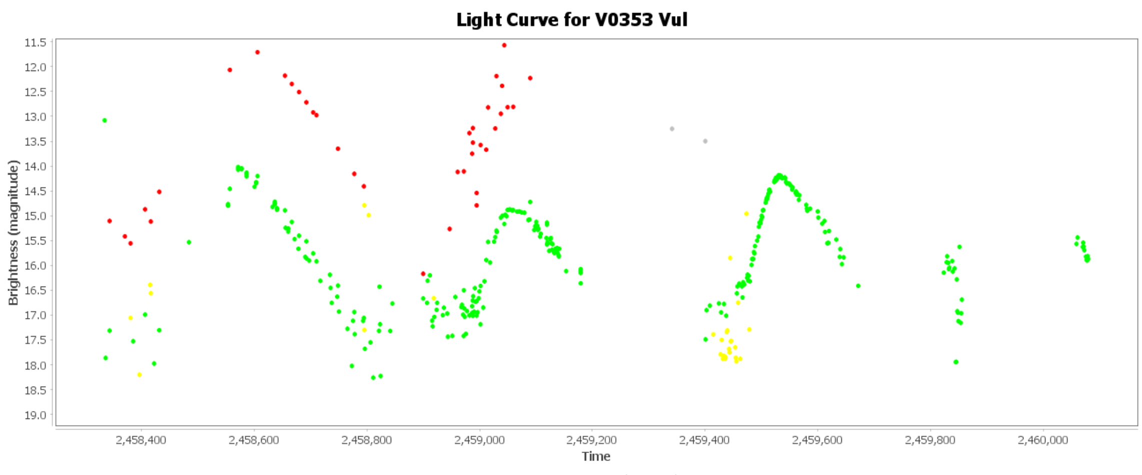
Light Curve for V0353 Vul
Brightness (magnitude)
Time
Cousins R
Discrepant
Fainter Than
Johnson V

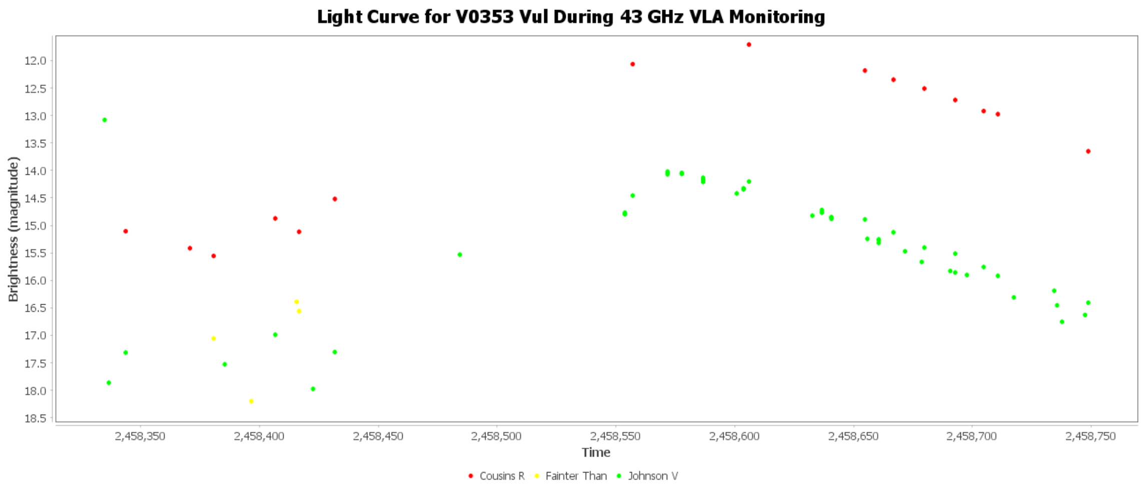
Light Curve for V0353 Vul During 43 GHz VLA Monitoring
Brightness (magnitude)
Time
Cousins R
Fainter Than
Johnson V

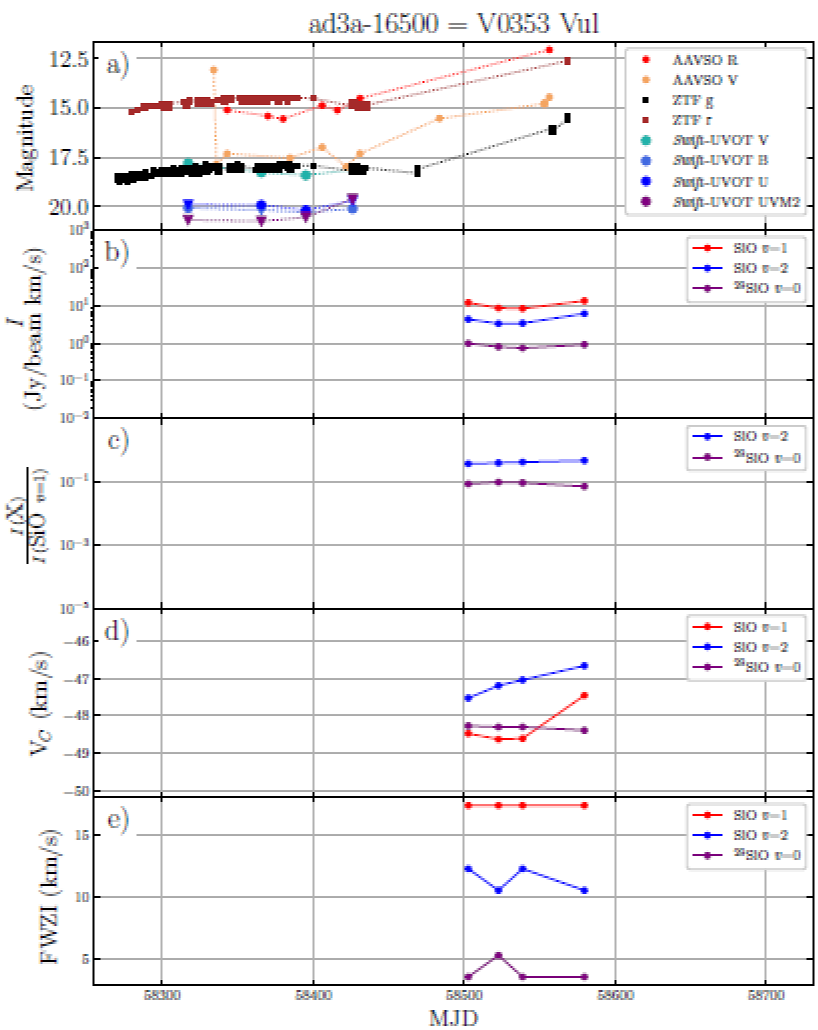
ad3a-16500 = V0353 Vul
Magnitude
AAVSO R
AAVSO V
ZTF g
ZTF r
Swift-UVOT V
Swift-UVOT B
Swift-UVOT U
Swift-UVOT UVM2
I (Jy/beam km/s)
SiO v=1
SiO v=2
29SiO v=0
V_C (km/s)
FWZI (km/s)
MJD

SX Cyg

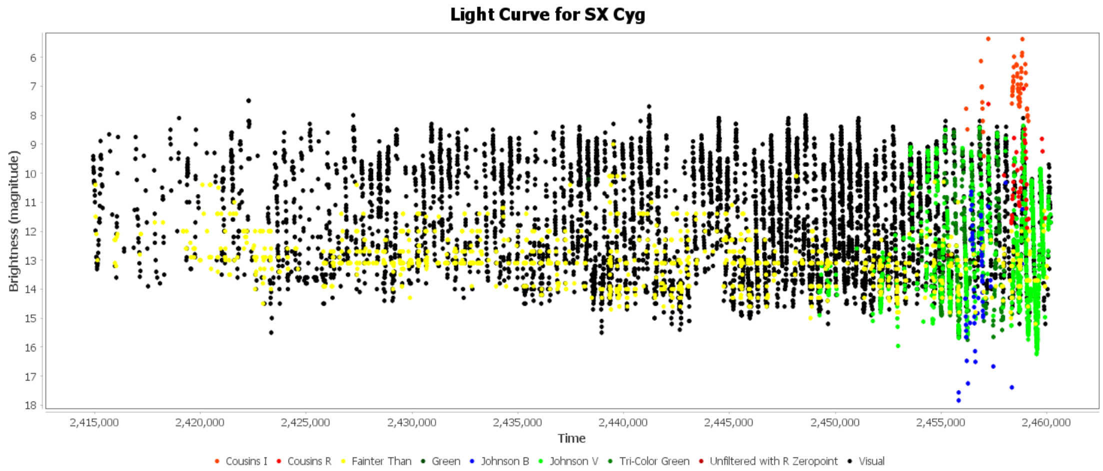
Light Curve for SX Cyg
Brightness (magnitude)
Time
2,415,000
2,420,000
2,425,000
2,430,000
2,435,000
2,440,000
2,445,000
2,450,000
2,455,000
2,460,000
Cousins I
Cousins R
Fainter Than
Green
Johnson B
Johnson V
Tri-Color Green
Unfiltered with R Zeropoint
Visual

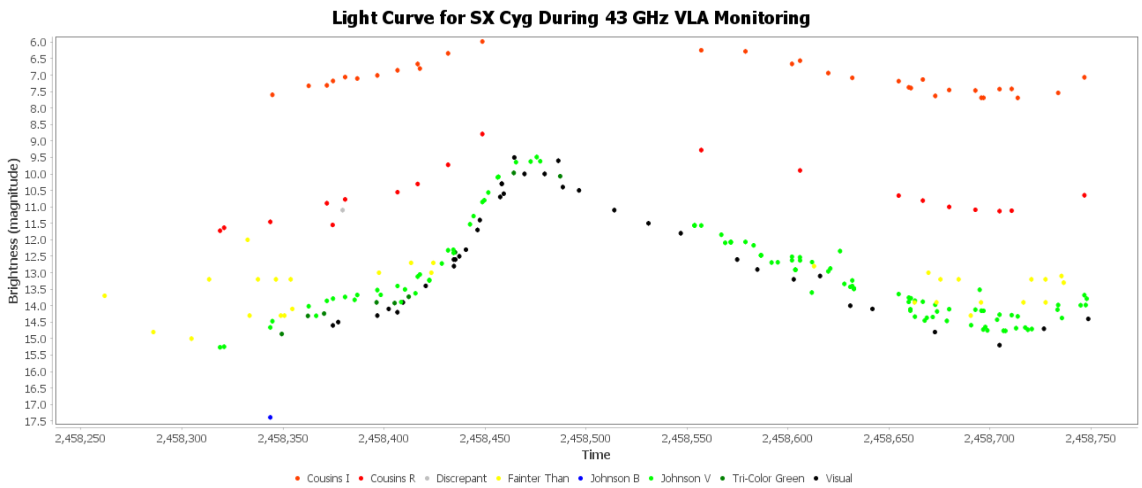
Light Curve for SX Cyg During 43 GHz VLA Monitoring
Brightness (magnitude)
Time
2,458,250
2,458,300
2,458,350
2,458,400
2,458,450
2,458,500
2,458,550
2,458,600
2,458,650
2,458,700
2,458,750
Cousins I
Cousins R
Discrepant
Fainter Than
Johnson B
Johnson V
Tri-Color Green
Visual

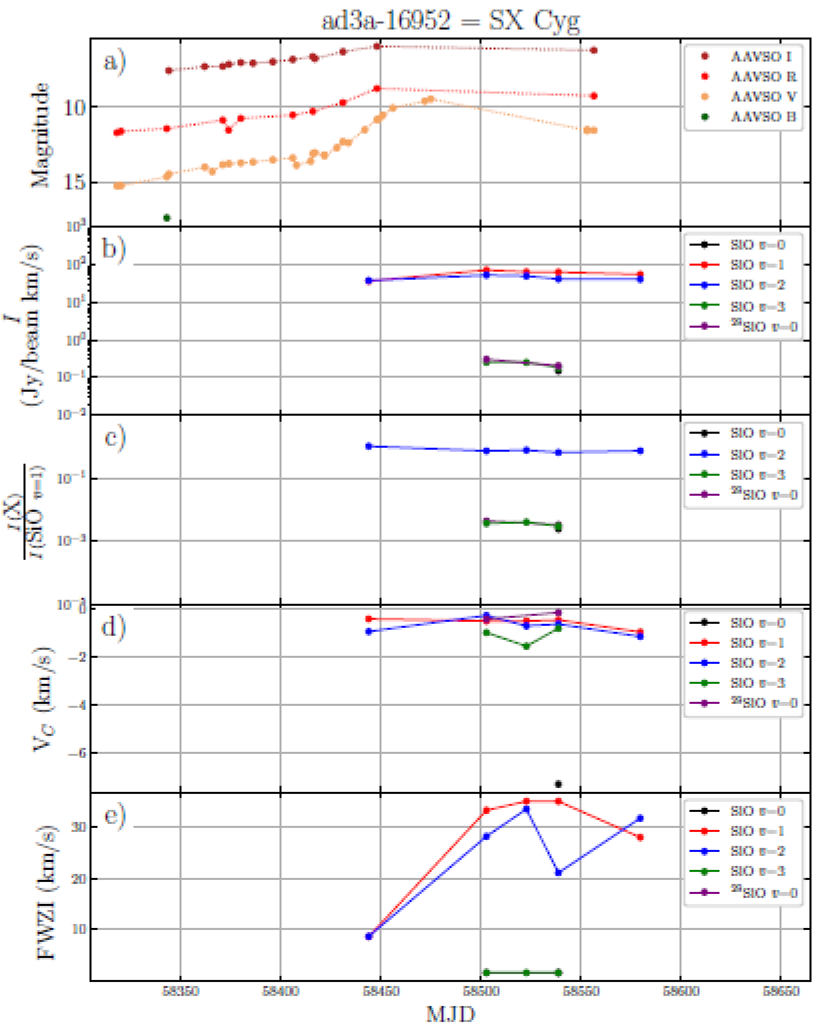
ad3a-16952 = SX Cyg
a)
b)
c)
d)
e)
Magnitude
I (Jy/beam km/s)
$\frac{I(X)}{I(\text{SiO } v=1)}$
V_C (km/s)
FWZI (km/s)
MJD
AAVSO I
AAVSO R
AAVSO V
AAVSO B
SiO v=0
SiO v=1
SiO v=2
SiO v=3
^{29}SiO v=0
58350
58400
58450
58500
58550
58600
58650

AU Cyg

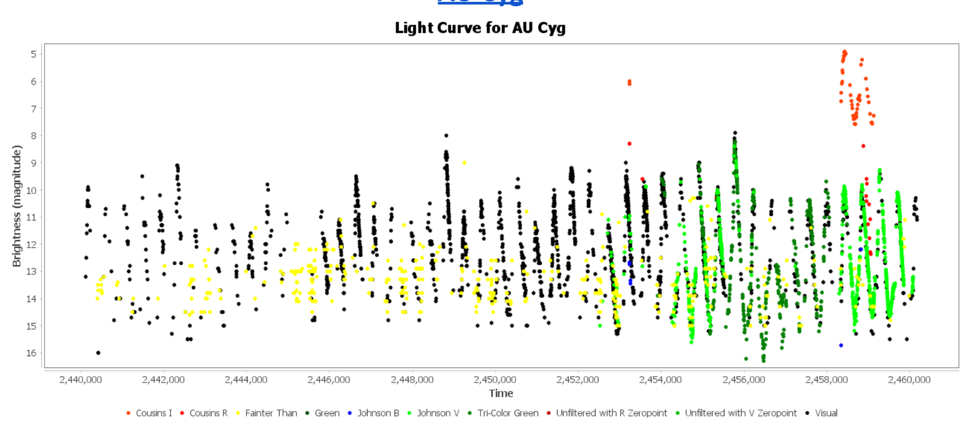
Light Curve for AU Cyg
Brightness (magnitude)
Time
Cousins I
Cousins R
Fainter Than
Green
Johnson B
Johnson V
Tri-Color Green
Unfiltered with R Zeropoint
Unfiltered with V Zeropoint
Visual
2,440,000
2,442,000
2,444,000
2,446,000
2,448,000
2,450,000
2,452,000
2,454,000
2,456,000
2,458,000
2,460,000

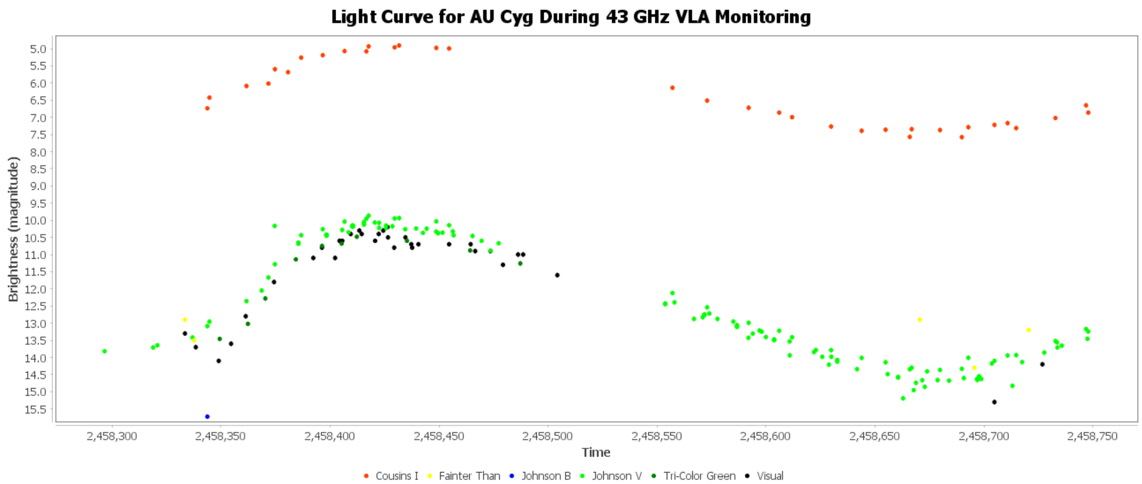

Light Curve for AU Cyg During 43 GHz VLA Monitoring
Brightness (magnitude)
Time
Cousins I
Fainter Than
Johnson B
Johnson V
Tri-Color Green
Visual

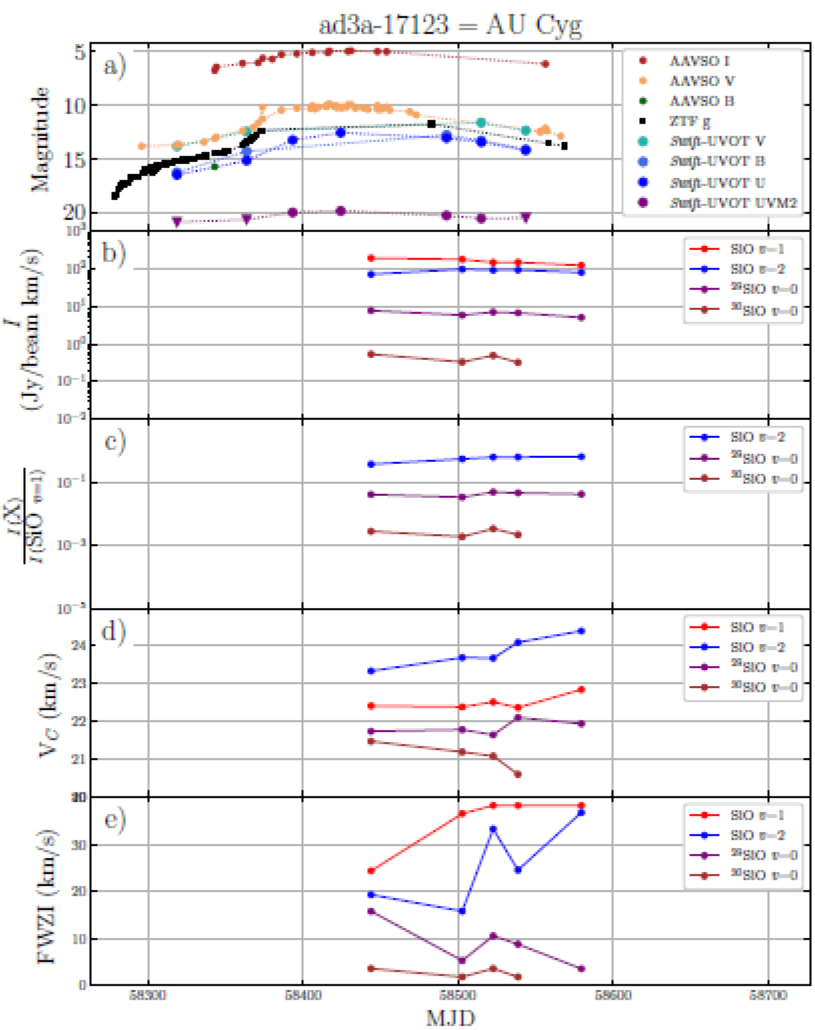

ad3a-17123 = AU Cyg
a)
b)
c)
d)
e)
Magnitude
AAVSO I
AAVSO V
AAVSO B
ZTF g
Swift-UVOT V
Swift-UVOT B
Swift-UVOT U
Swift-UVOT UVM2
I (Jy/beam km/s)
SiO v=1
SiO v=2
29SiO v=0
30SiO v=0
I(X) / I(SiO v=1)
V_C (km/s)
FWZI (km/s)
MJD

V1655 Cyg

Light Curve for V1655 Cyg

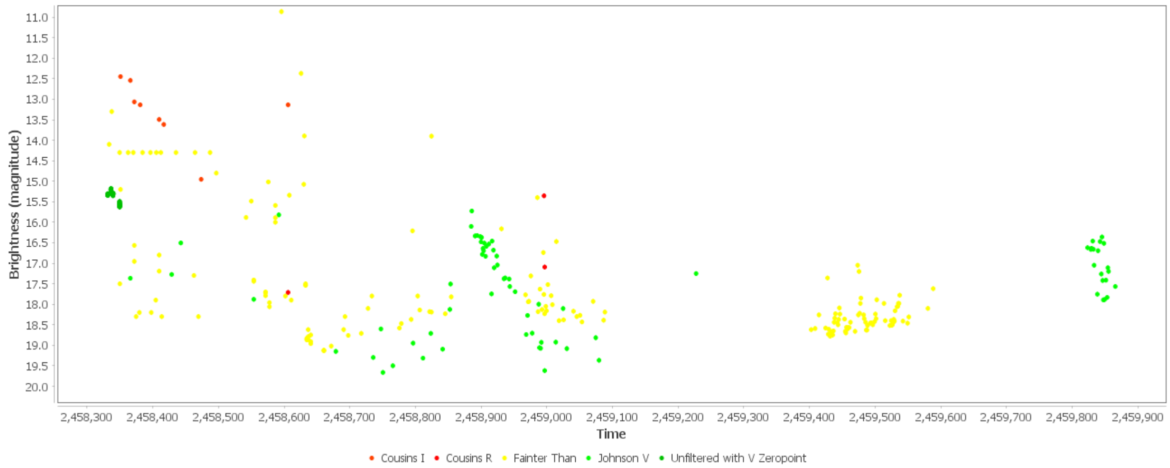

Light Curve for V1655 Cyg During 43 GHz VLA Monitoring

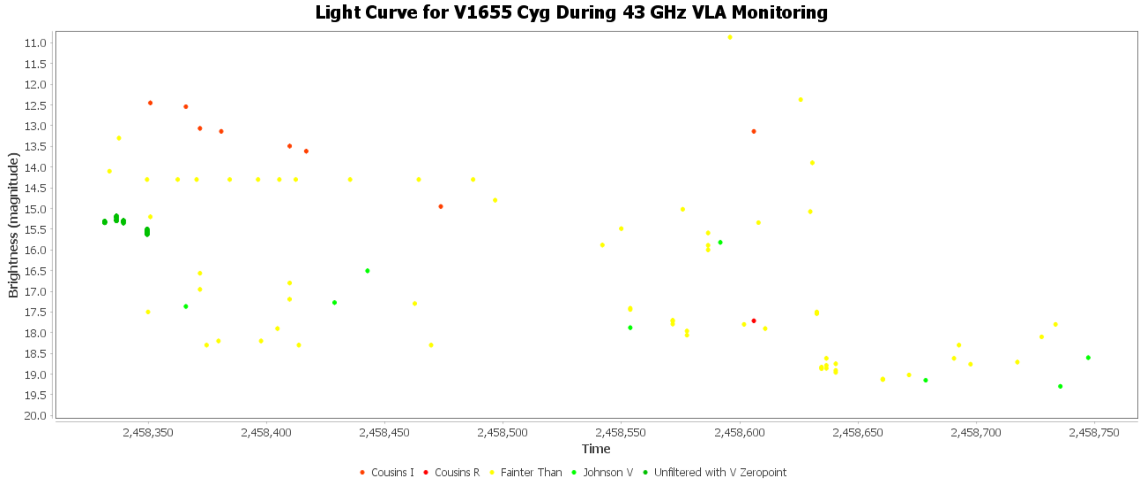

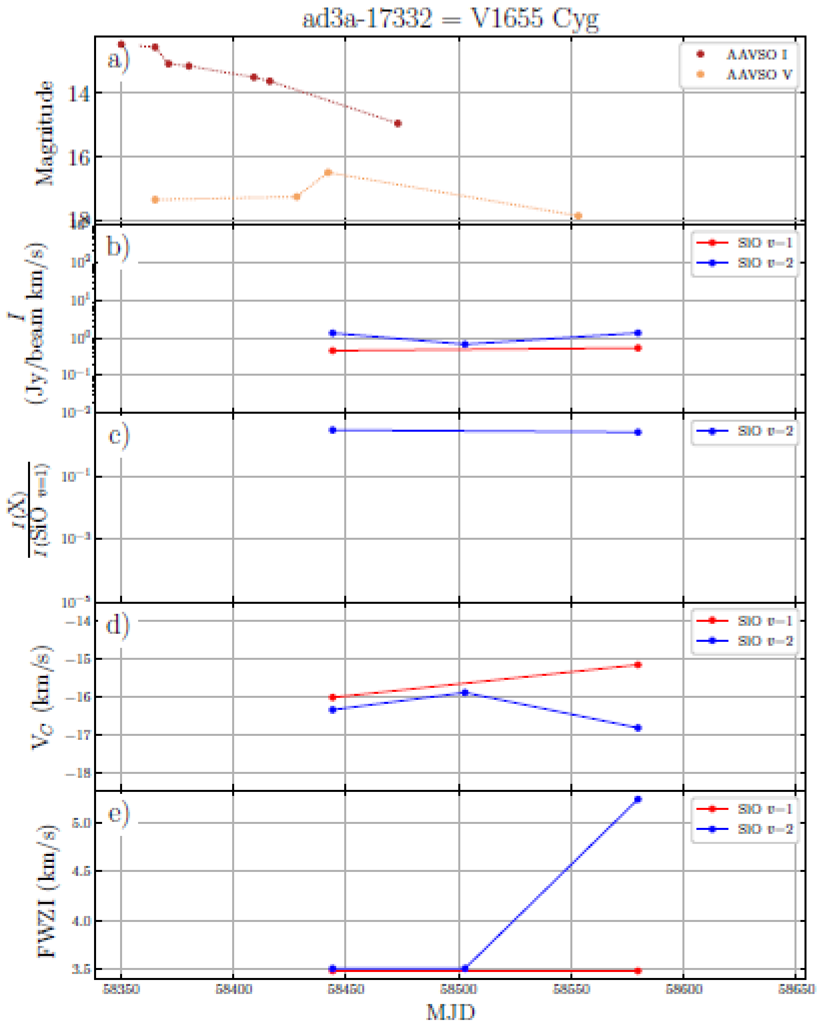

NSVS J2041274+511326

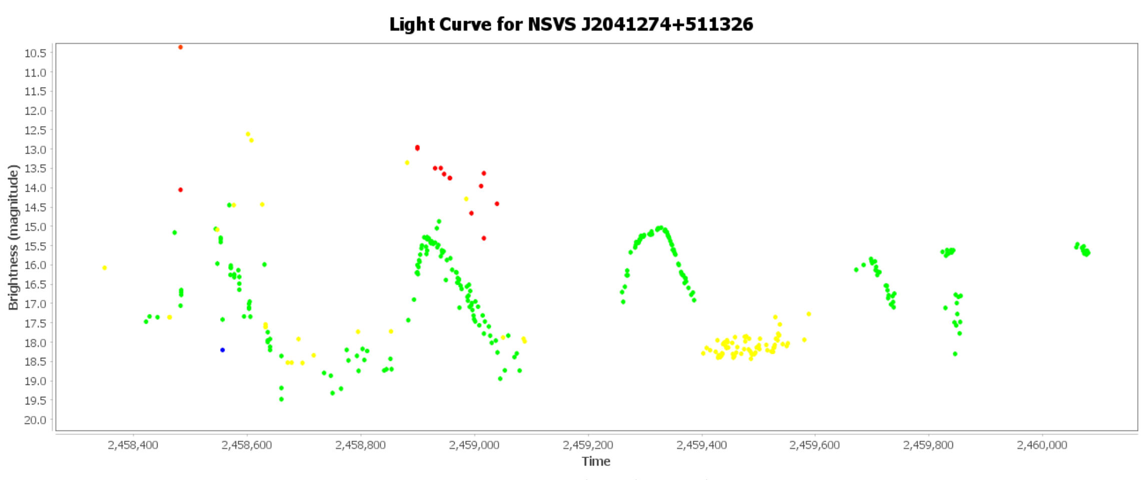

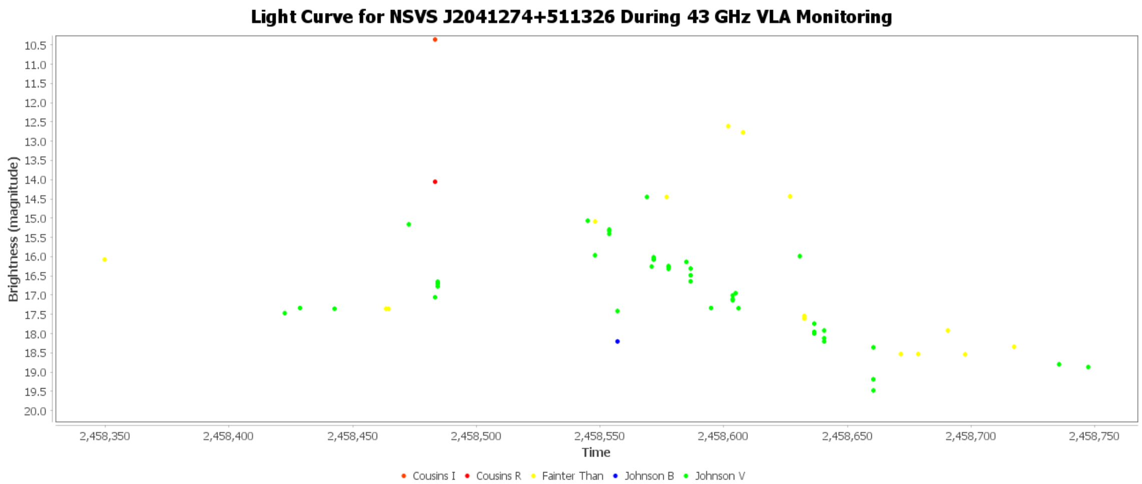
Light Curve for NSVS J2041274+511326 During 43 GHz VLA Monitoring
Brightness (magnitude)
Time
Cousins I
Cousins R
Fainter Than
Johnson B
Johnson V

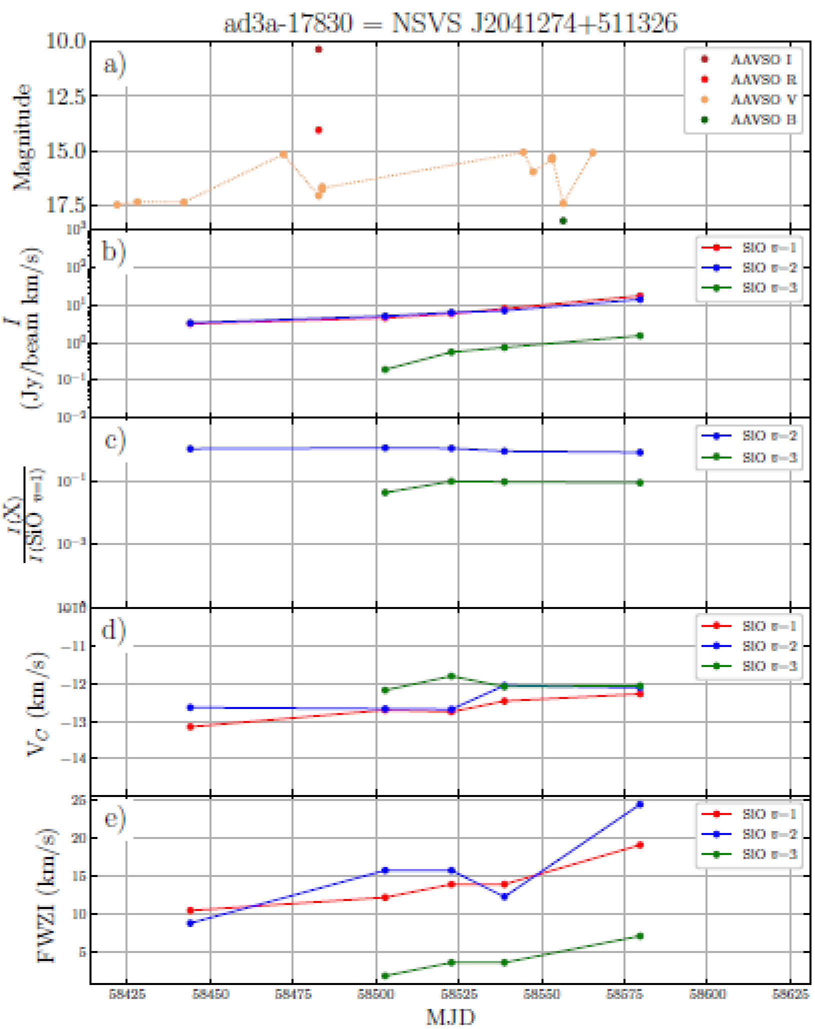
ad3a-17830 = NSVS J2041274+511326
Magnitude
AAVSO I
AAVSO R
AAVSO V
AAVSO B
SiO v=1
SiO v=2
SiO v=3
V_C (km/s)
FWZI (km/s)
MJD

DR Cyg

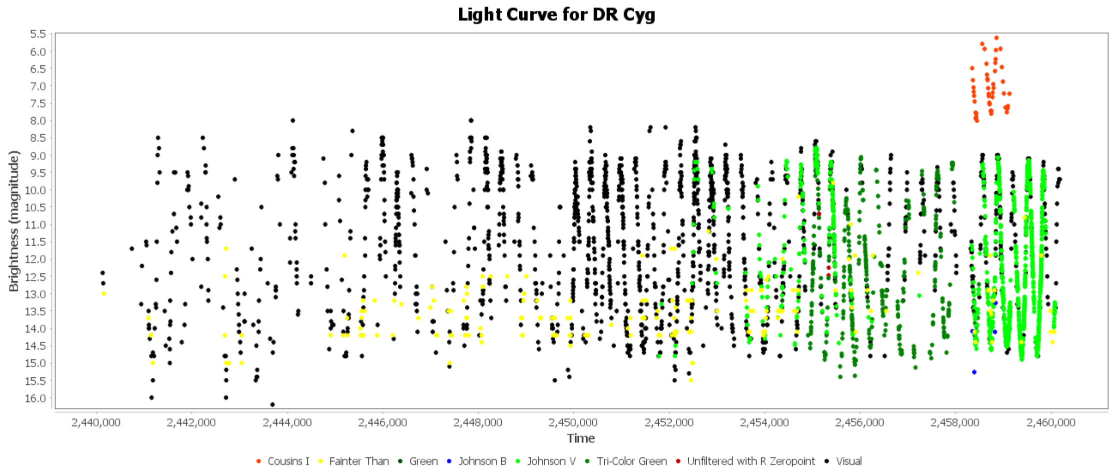
Light Curve for DR Cyg
Brightness (magnitude)
Time
Cousins I
Fainter Than
Green
Johnson B
Johnson V
Tri-Color Green
Unfiltered with R Zeropoint
Visual

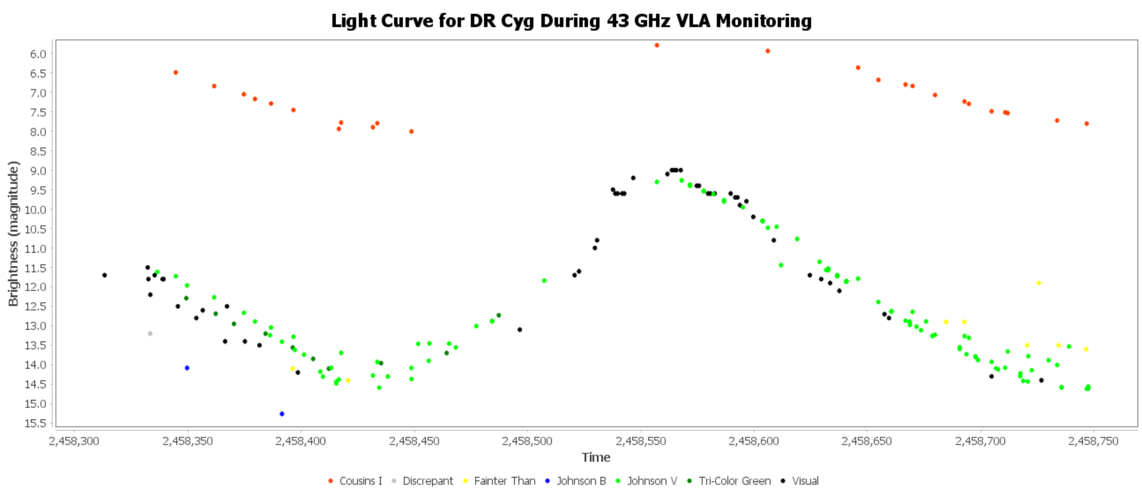
Light Curve for DR Cyg During 43 GHz VLA Monitoring
Brightness (magnitude)
Time
Cousins I
Discrepant
Fainter Than
Johnson B
Johnson V
Tri-Color Green
Visual

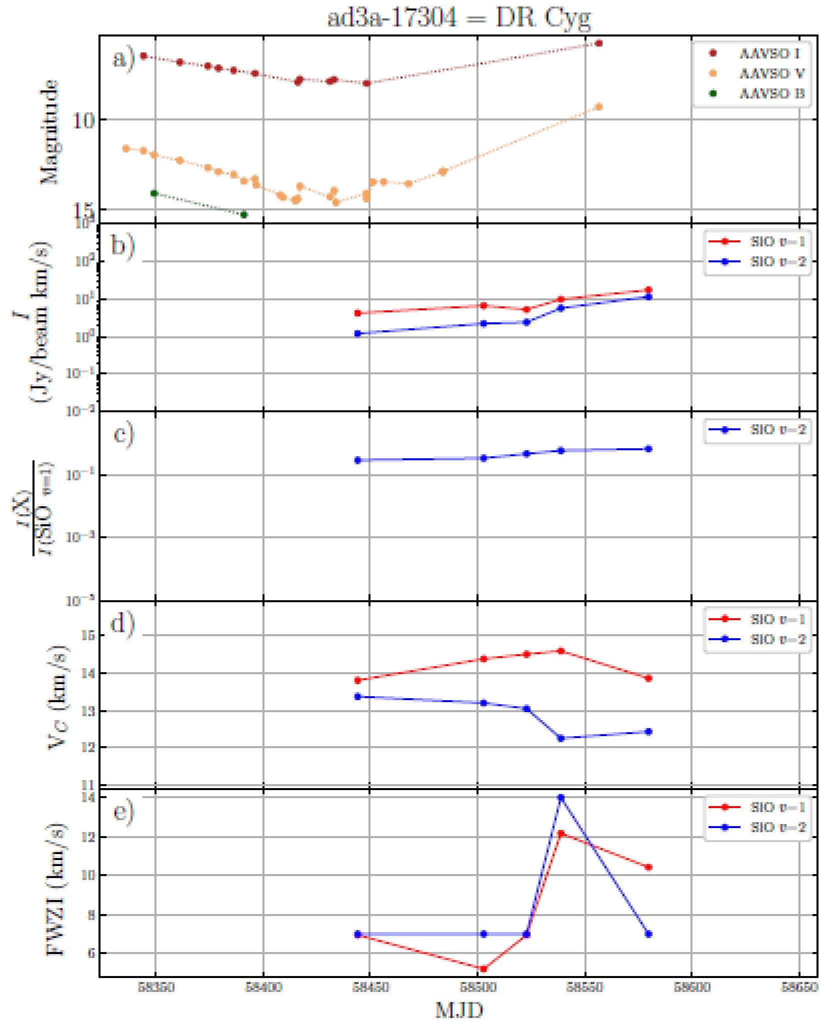

V0750 Cyg

Light Curve for V0750 Cyg

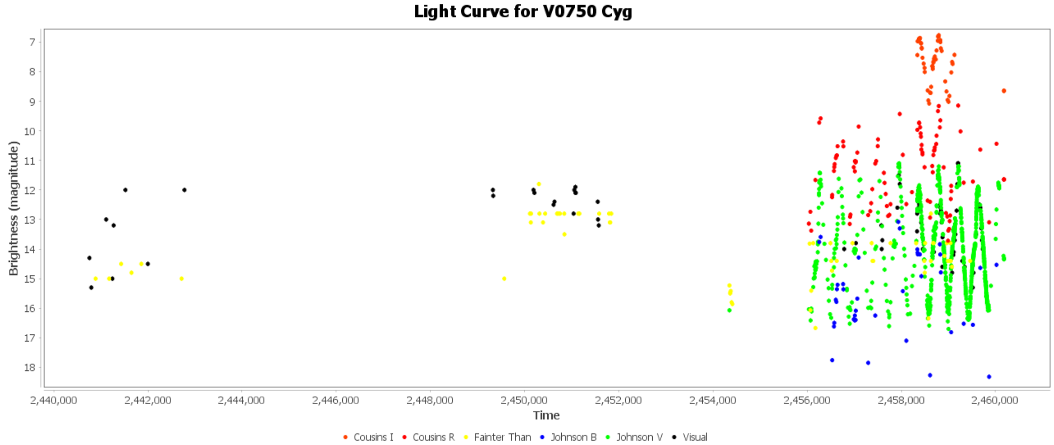

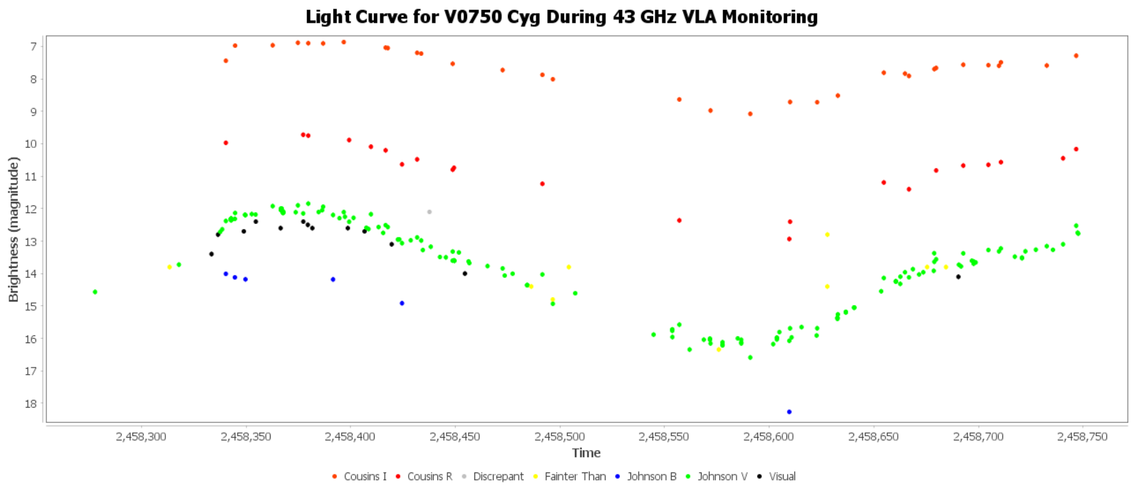
Light Curve for V0750 Cyg During 43 GHz VLA Monitoring
Brightness (magnitude)
Time
Cousins I
Cousins R
Discrepant
Fainter Than
Johnson B
Johnson V
Visual

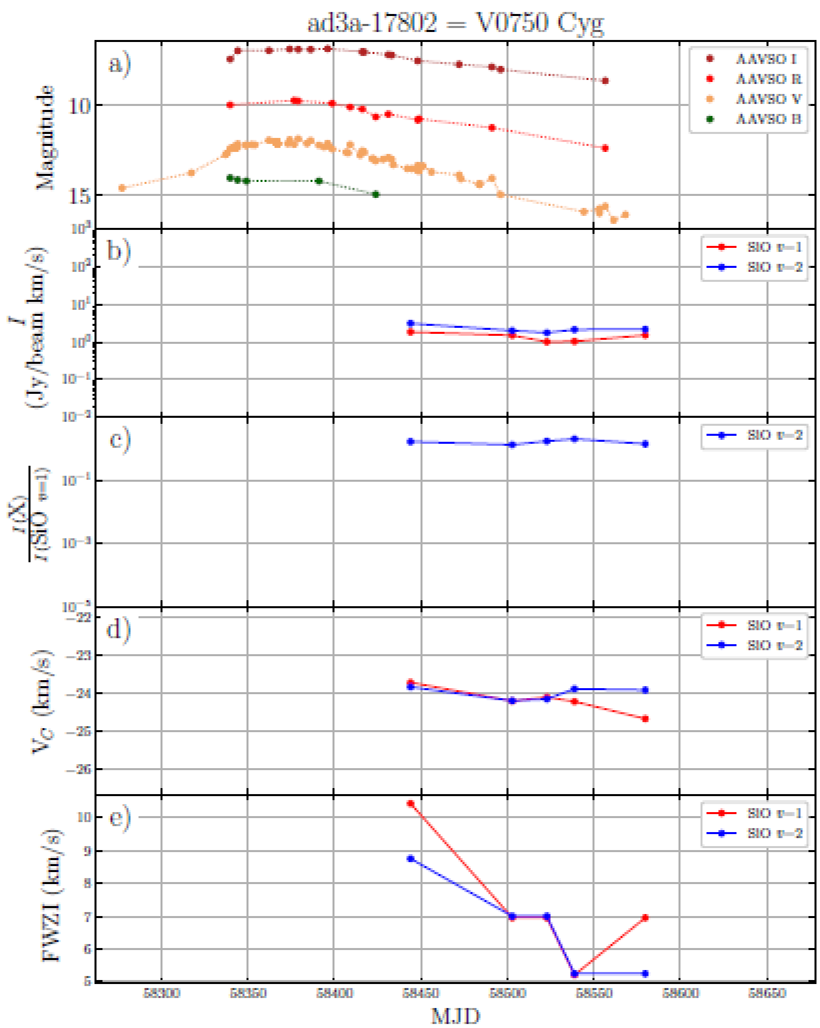
ad3a-17802 = V0750 Cyg
a)
Magnitude
AAVSO I
AAVSO R
AAVSO V
AAVSO B
b)
I (Jy/beam km/s)
SiO v=1
SiO v=2
c)
I(X) / I(SiO v=1)
d)
V_C (km/s)
e)
FWZI (km/s)
MJD

W Cep

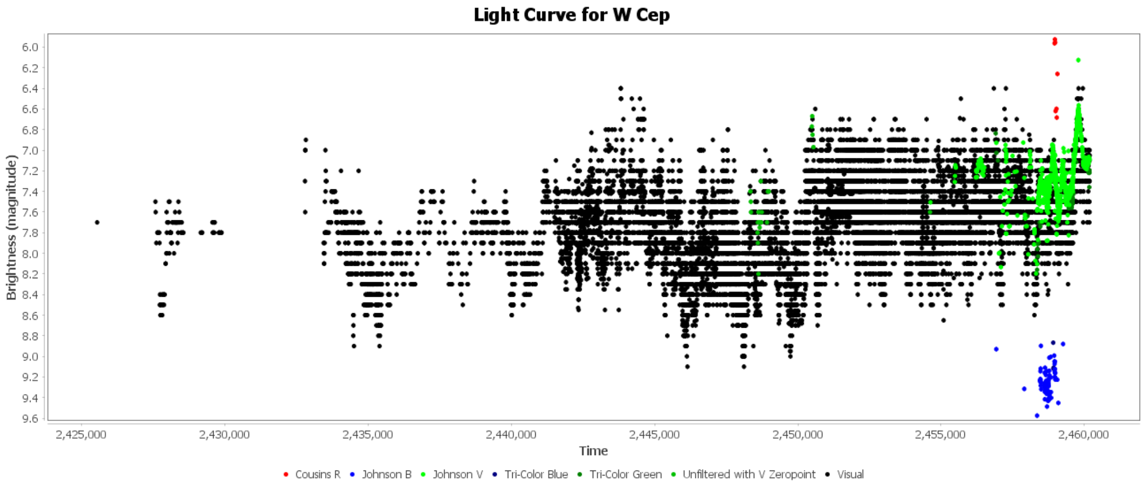
Light Curve for W Cep
Brightness (magnitude)
Time
Cousins R
Johnson B
Johnson V
Tri-Color Blue
Tri-Color Green
Unfiltered with V Zeropoint
Visual

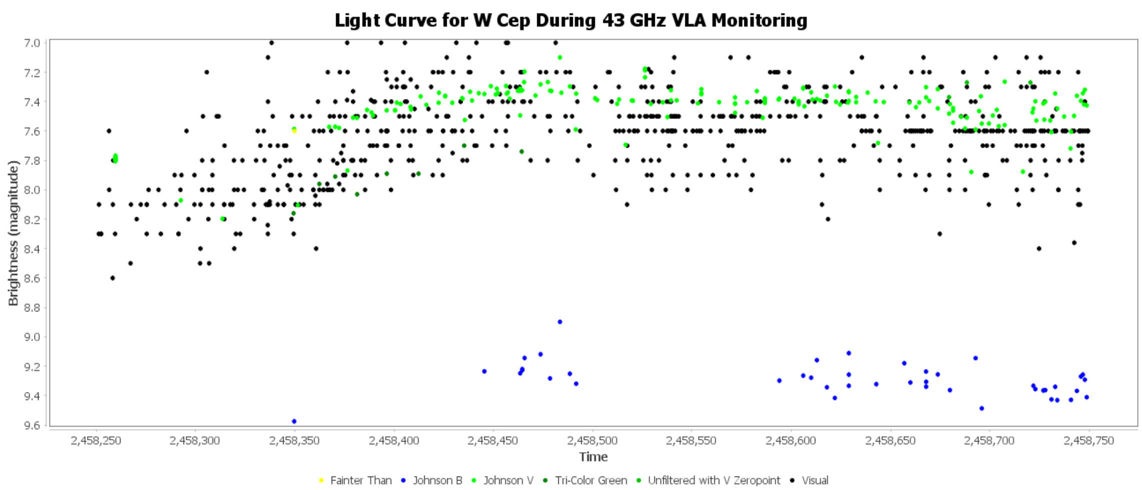
Light Curve for W Cep During 43 GHz VLA Monitoring
Brightness (magnitude)
Time
Fainter Than
Johnson B
Johnson V
Tri-Color Green
Unfiltered with V Zeropoint
Visual

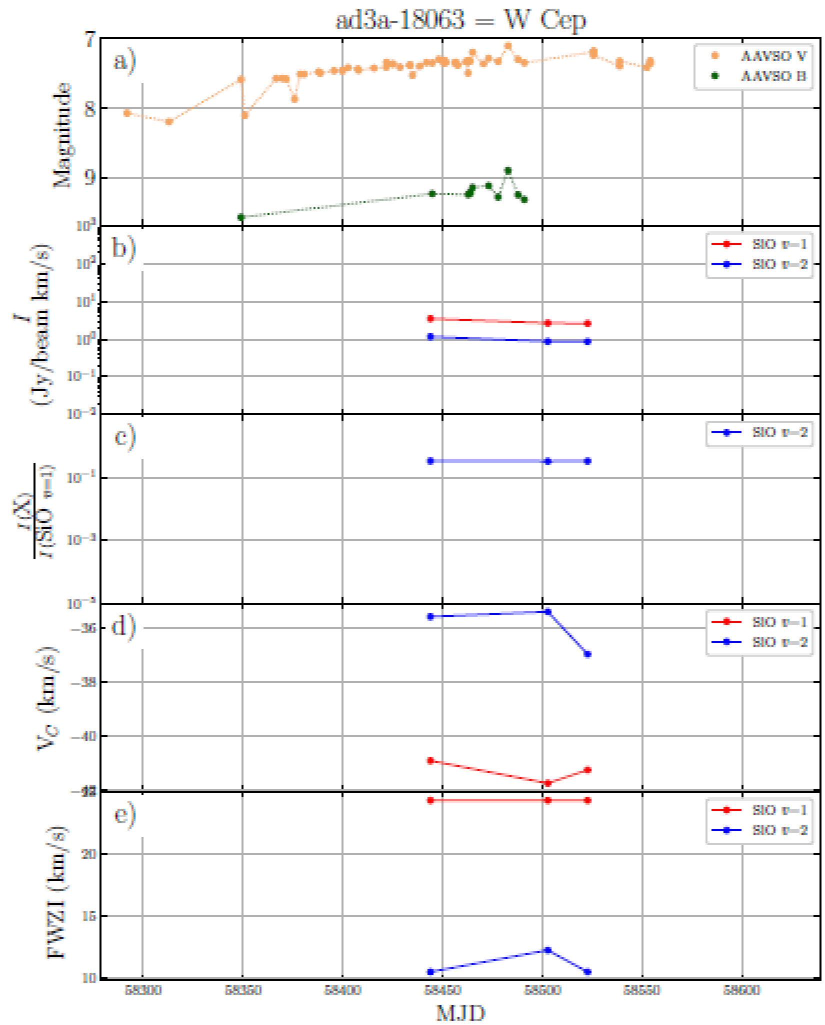
ad3a-18063 = W Cep
a)
b)
c)
d)
e)
Magnitude
AAVSO V
AAVSO B
I (Jy/beam km/s)
SiO v=1
SiO v=2
I(X) / I(SiO v=1)
V_C (km/s)
FWZI (km/s)
MJD

VX Cep

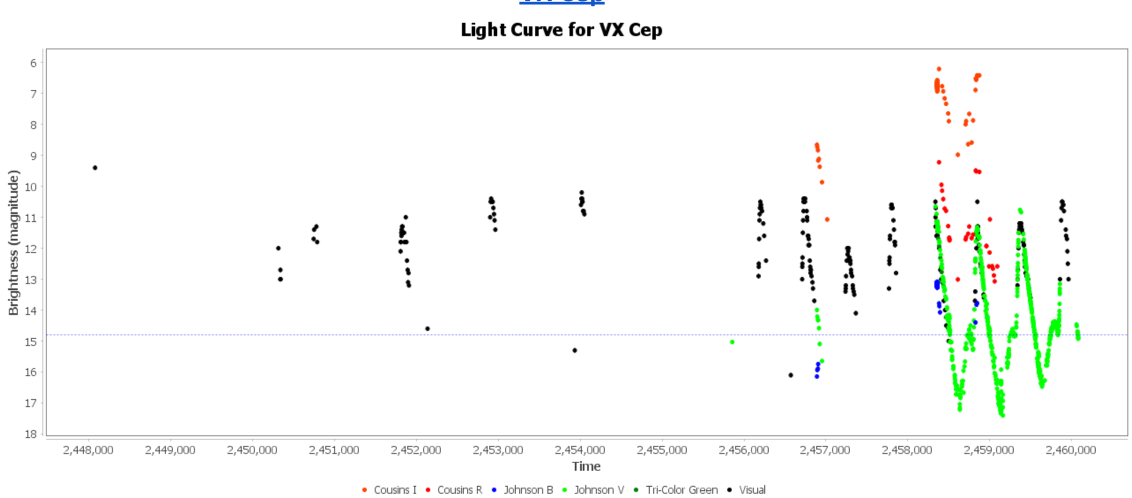
Light Curve for VX Cep
Brightness (magnitude)
Time
Cousins I
Cousins R
Johnson B
Johnson V
Tri-Color Green
Visual

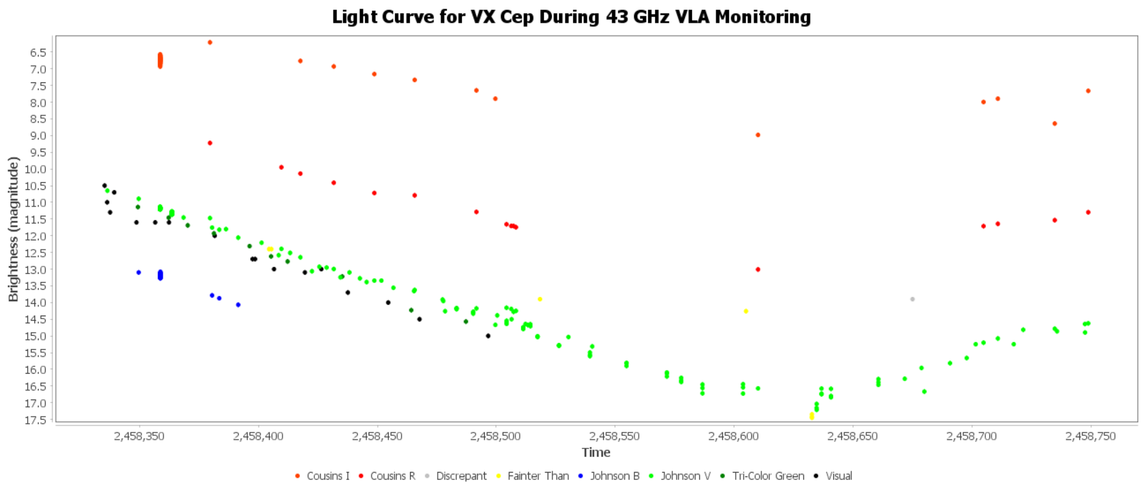

Light Curve for VX Cep During 43 GHz VLA Monitoring
Brightness (magnitude)
Time
Cousins I
Cousins R
Discrepant
Fainter Than
Johnson B
Johnson V
Tri-Color Green
Visual

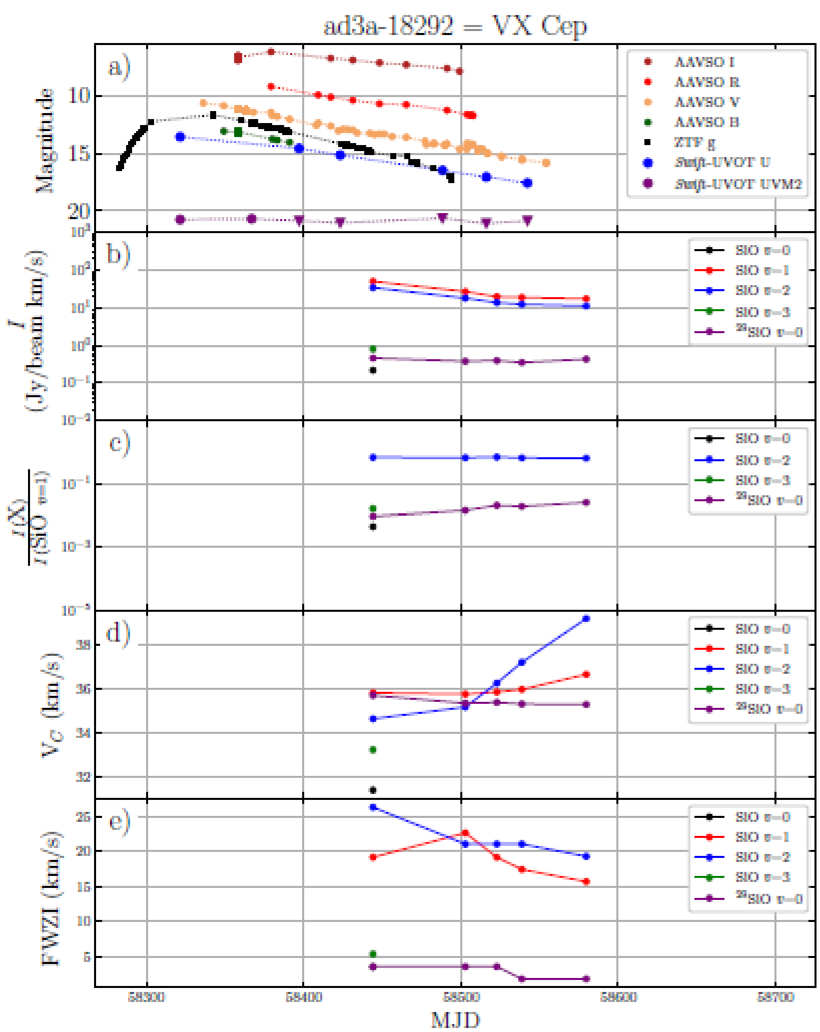

ad3a-18292 = VX Cep
a)
b)
c)
d)
e)
Magnitude
AAVSO I
AAVSO R
AAVSO V
AAVSO B
ZTF g
Swift-UVOT U
Swift-UVOT UVM2
I (Jy/beam km/s)
SiO v=0
SiO v=1
SiO v=2
SiO v=3
29SiO v=0
I(X) / I(SiO v=1)
V_C (km/s)
FWZI (km/s)
MJD

V0850 Cas

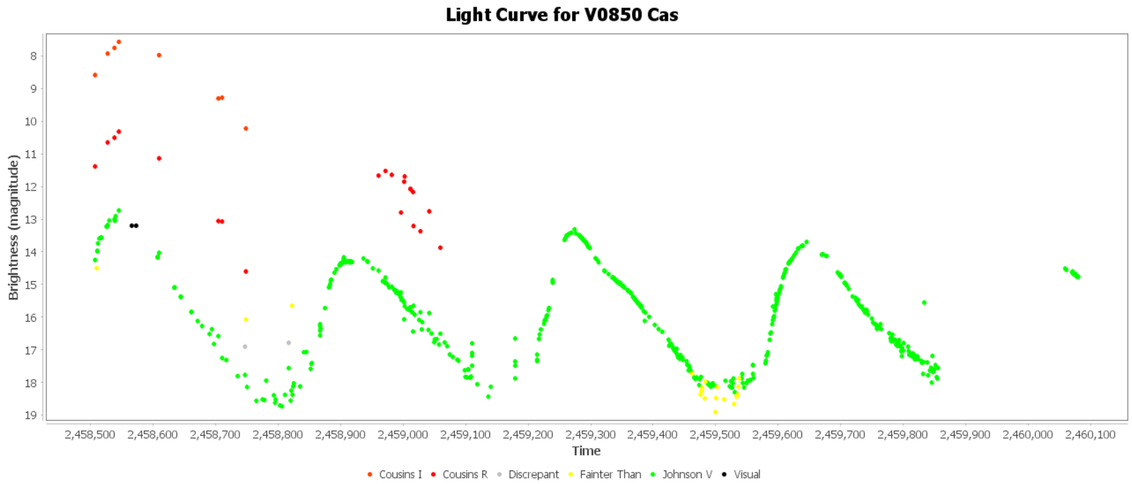
Light Curve for V0850 Cas
Brightness (magnitude)
Time
Cousins I
Cousins R
Discrepant
Fainter Than
Johnson V
Visual

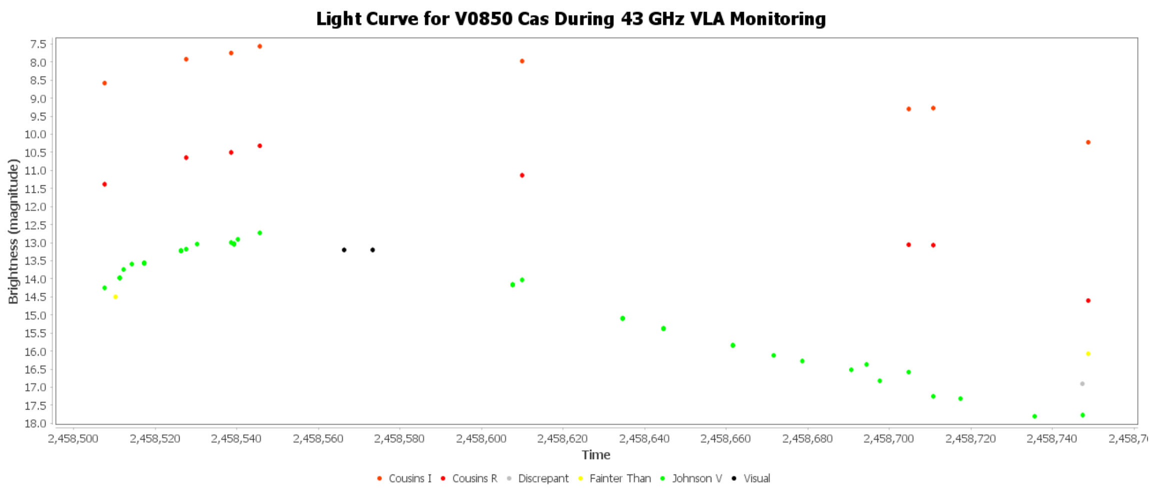
Light Curve for V0850 Cas During 43 GHz VLA Monitoring
Brightness (magnitude)
Time
Cousins I
Cousins R
Discrepant
Fainter Than
Johnson V
Visual

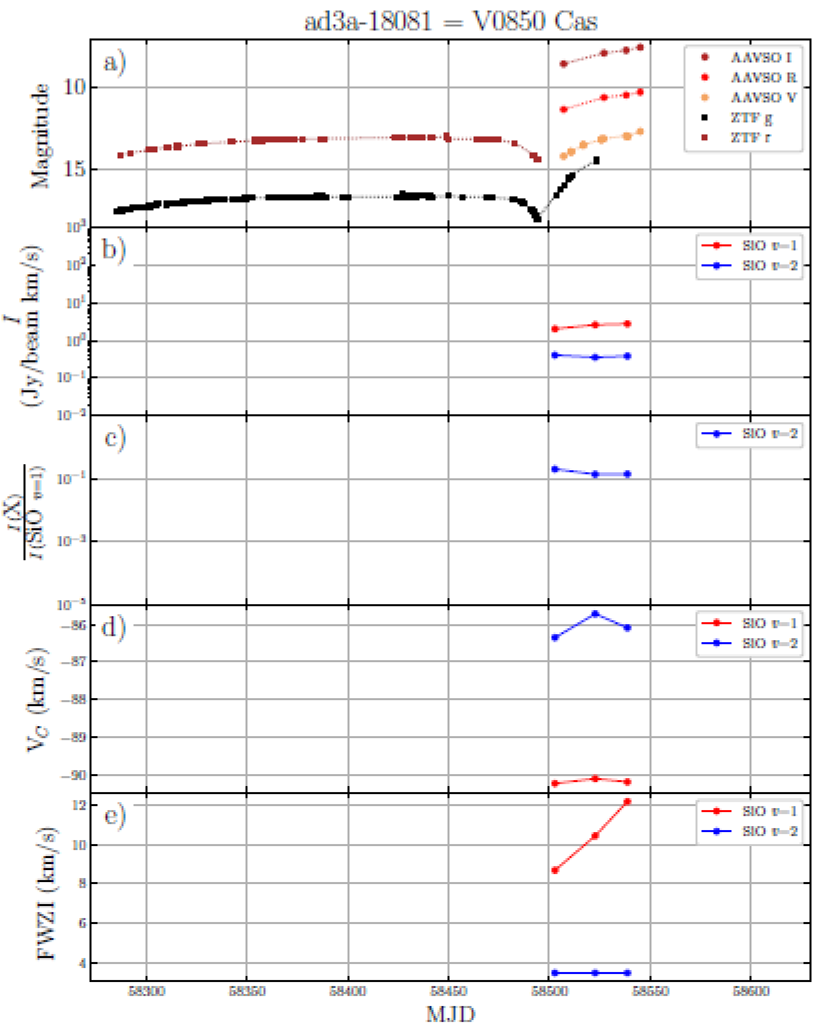
ad3a-18081 = V0850 Cas
a)
b)
c)
d)
e)
Magnitude
AAVSO I
AAVSO R
AAVSO V
ZTF g
ZTF r
SiO v=1
SiO v=2
FWZI (km/s)
MJD

AL Cep

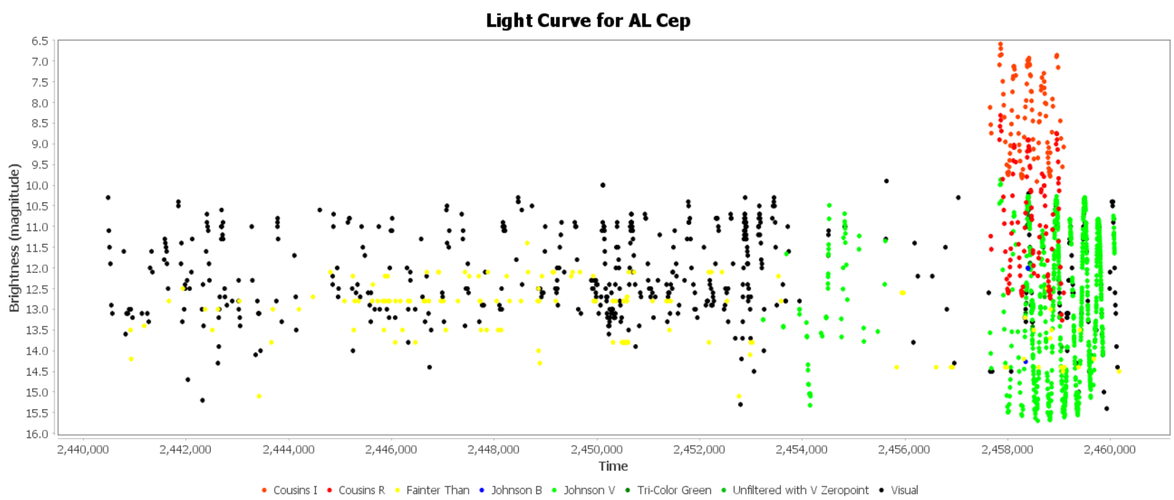
Light Curve for AL Cep
Brightness (magnitude)
Time
Cousins I
Cousins R
Fainter Than
Johnson B
Johnson V
Tri-Color Green
Unfiltered with V Zeropoint
Visual

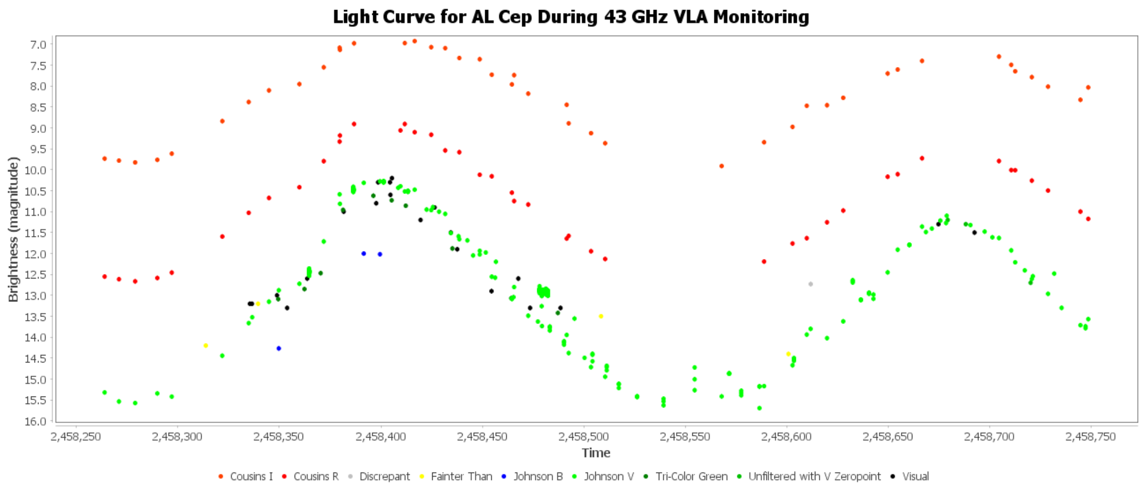

Light Curve for AL Cep During 43 GHz VLA Monitoring
Brightness (magnitude)
Time
Cousins I
Cousins R
Discrepant
Fainter Than
Johnson B
Johnson V
Tri-Color Green
Unfiltered with V Zeropoint
Visual

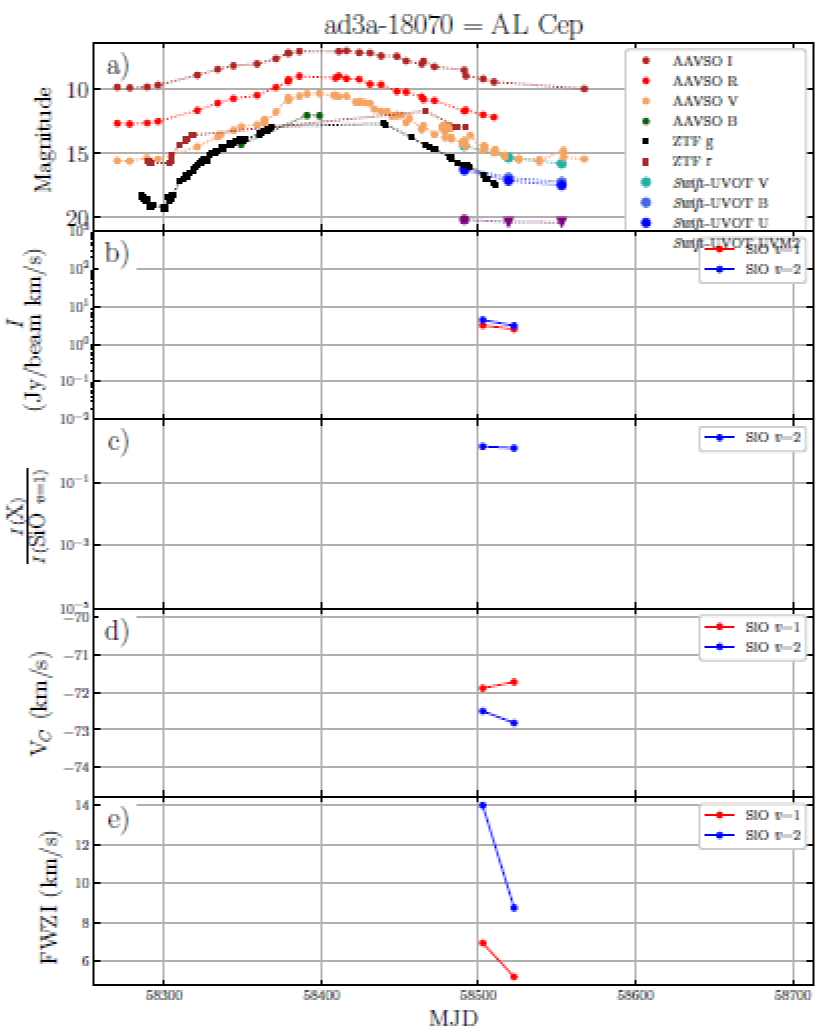

ad3a-18070 = AL Cep
Magnitude
AAVSO I
AAVSO R
AAVSO V
AAVSO B
ZTF g
ZTF r
Swift-UVOT V
Swift-UVOT B
Swift-UVOT U
I (Jy/beam km/s)
SiO v=1
SiO v=2
V_C (km/s)
FWZI (km/s)
MJD

V Cas

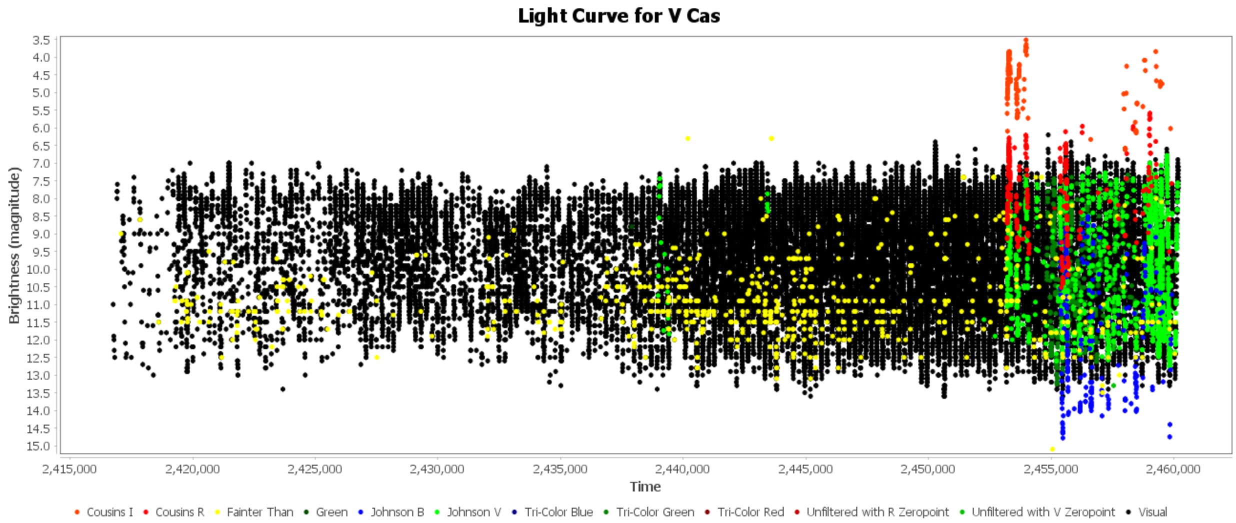

Light Curve for V Cas
Brightness (magnitude)
Time
Cousins I
Cousins R
Fainter Than
Green
Johnson B
Johnson V
Tri-Color Blue
Tri-Color Green
Tri-Color Red
Unfiltered with R Zeropoint
Unfiltered with V Zeropoint
Visual

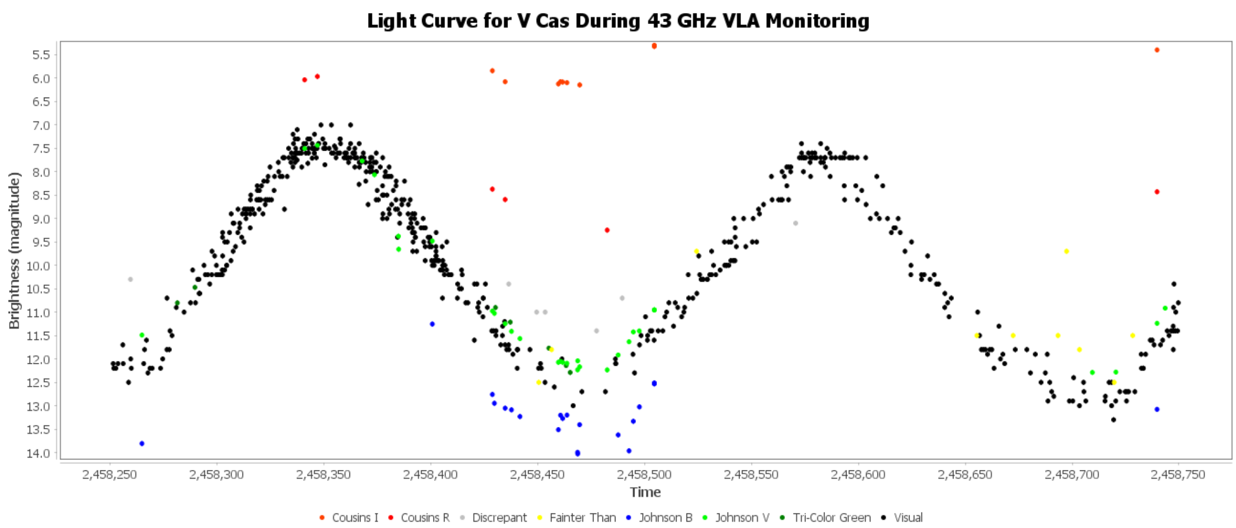

Light Curve for V Cas During 43 GHz VLA Monitoring
Brightness (magnitude)
Time
Cousins I
Cousins R
Discrepant
Fainter Than
Johnson B
Johnson V
Tri-Color Green
Visual

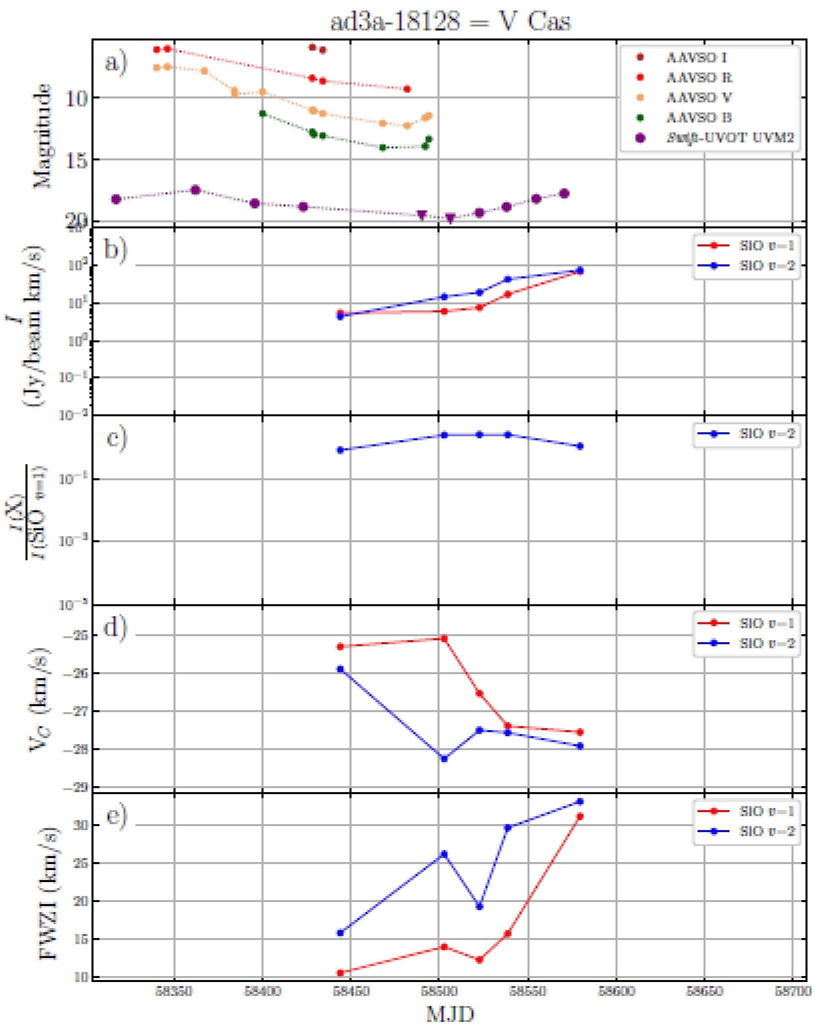
ad3a-18128 = V Cas
a)
Magnitude
AAVSO I
AAVSO R
AAVSO V
AAVSO B
Swift-UVOT UVM2
b)
I (Jy/beam km/s)
SiO v=1
SiO v=2
c)
I(X) / I(SiO v=1)
d)
V_C (km/s)
e)
FWZI (km/s)
MJD

V0657 Cas

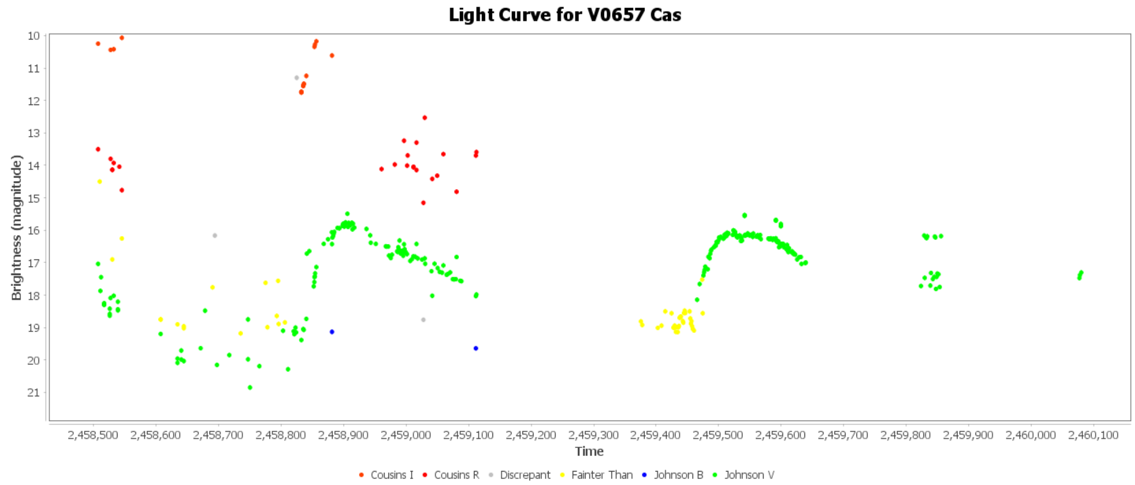

Light Curve for V0657 Cas
Brightness (magnitude)
Time
Cousins I
Cousins R
Discrepant
Fainter Than
Johnson B
Johnson V

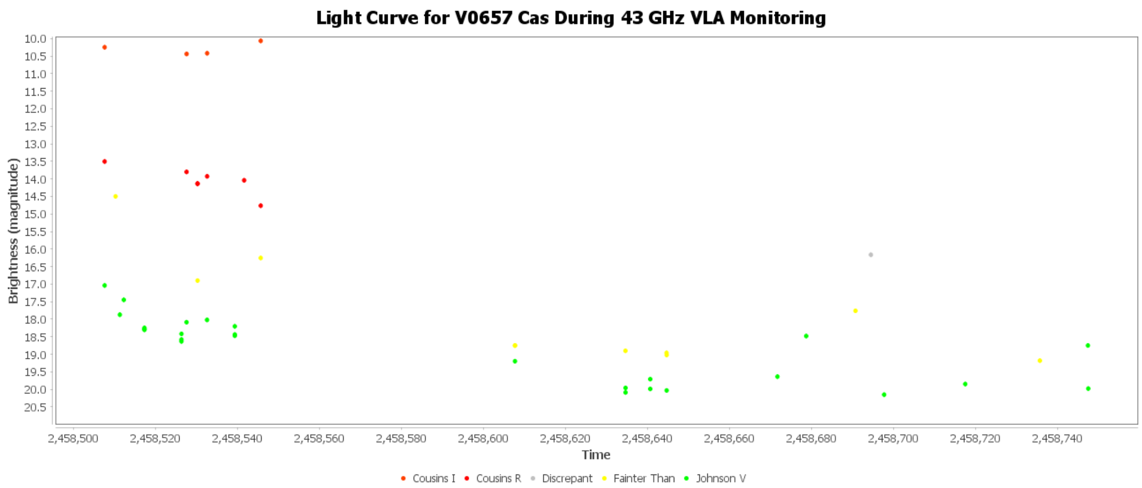

Light Curve for V0657 Cas During 43 GHz VLA Monitoring
Brightness (magnitude)
Time
Cousins I
Cousins R
Discrepant
Fainter Than
Johnson V

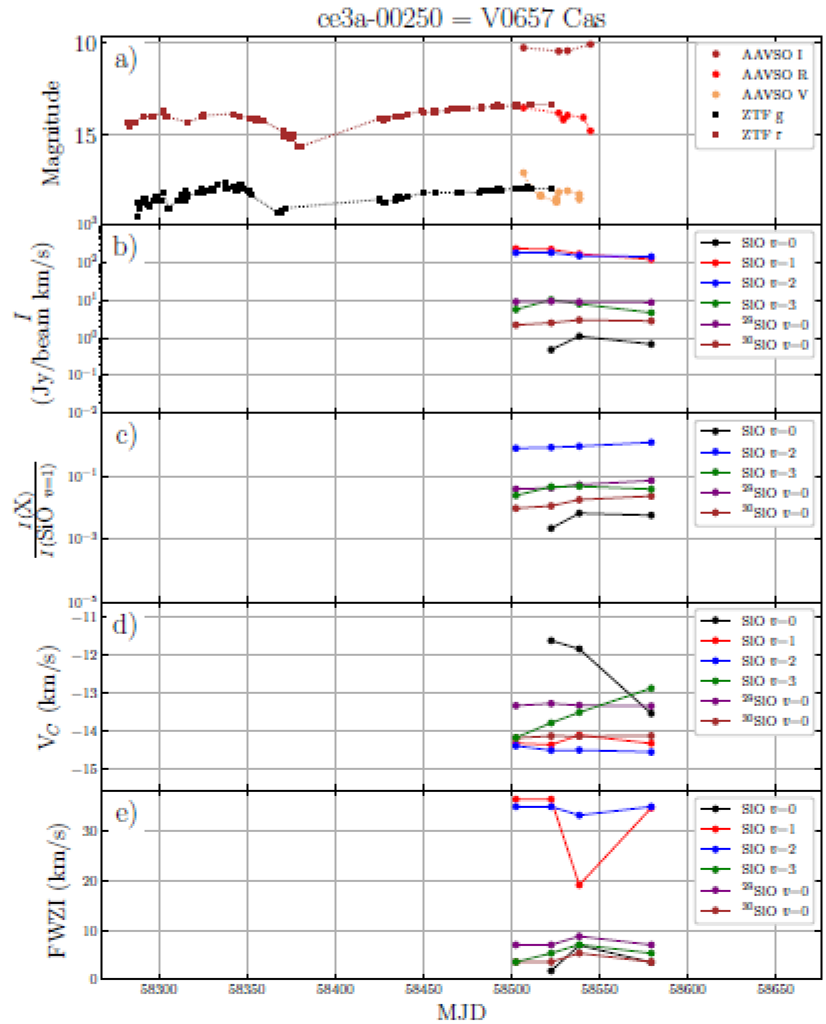

3. Discussion and Conclusions

The American Association of Variable Star Observers **(**Kloppenborg 2022, American Association of Variable Star Observers (https://aavso.org)) and the University of New Mexico (Stroh, M. "Circumstellar SiO Masers in the Bulge Asymmetries and Dynamical Evolution Survey", 2019, https://digitalrepository.unm.edu/phyc_etds/216) participated in a cooperative effort to study SiO maser emissions. The maser emissions were observed with the Jansky Very Large Array (JVLA) by the University of New Mexico. This study surveyed red giant sources in the Galactic bulge and inner Galaxy for SiO maser emission at 7mm and 3mm wavelengths (43 GHz and 86 GHz). At these wavelengths, observations are not hindered by extinction, and extremely accurate stellar velocities (< 1 km/s) and positions can be determined. The survey targeted approximately 28,000 red giant SiO maser sources. In total, twenty Mira Long Period Variable (LPV) stars were studied with the combination of AAVSO light curves and the VLA 43 GHz radio frequency observations. The particular stars selected were based on previous SiO observations as well as a good history of AAVSO coverage. These objects are outlined in Figure 1.

For each of the twenty Mira variables listed in Figure 1, three plots display pertinent optical and radio frequency information. These include the latest overall AAVSO light curve, the portion of the AAVSO light curve that corresponds to the time period in which the VLA was observing the maser activity, and the composite data from the University of New Mexico study. The composite data includes light curves from AAVSO as well as other sensor (e.g., the Swift spacecraft and the Zwicky Transient Facility (ZTF)) data in the top panel. The second panel shows Integrated Flux Density I (Jy/beam km/s), the third panel shows Integrated Flux Density relative to the SiO v=1 emission, the fourth panel shows the velocity centroid of the emission, and the fifth panel shows the full linewidth at zero maximum (i.e., the width of all emissions).

Since the time interval over which the 43 GHz VLA observations were performed (JD 2458249-JD 2458750 or May 10, 2018 - September 23, 2019) is just a small fraction of the overall light curve for the maser object (for example, JD 2414940-JD 2460185 or October 13, 1899 - August 29, 2023 for SX Cyg), it is difficult to draw any firm conclusions without more extensive VLA data. However, examining the AAVSO light curve corresponding to the time of the VLA maser observations as well as the AAVSO and other optical data shown in the top panel of the composite data (Swift and ZTF) indicates that there appears to be a general correlation between the optical data and the VLA intensity I (Jy/beam km/s) for all objects. In some cases, there is a strong correlation while in other cases the correlation is weak. Additionally, the integrated flux density relative to the SiO v=1 emission tracks the intensity I and the optical light curves.

References

Benn, D. 2012, “Algorithms + Observations = VStar”, JAAVSO, v40, n2, pp.852-866 (https://www.aavso.org/vstar) AAVSO VStar data analysis software.

Ferraz-Mello, S. 1981, Estimation of Periods From Unequally Spaced Observations, Astron. J., vol 86, p619. (https://adsabs.harvard.edu/full/1981AJ.....86..619F)

Kloppenborg 2022, American Association of Variable Star Observers (AAVSO) (https://aavso.org).

Kloppenborg 2022, American Association of Variable Star Observers (AAVSO) International Variable Star Index (VSX) (https://www.aavso.org/vsx/). This research has made use of the International Variable Star Index (VSX) database, operated at AAVSO, Cambridge, Massachusetts, USA.

Kloppenborg 2022, American Association of Variable Star Observers (AAVSO) Alert Notice 687.

Stroh, Michael Cullen. "Circumstellar SiO Masers in the Bulge Asymmetries and Dynamical Evolution Survey." (2019). https://digitalrepository.unm.edu/phyc_etds/216